Molecular mechanisms of metabolic regulation of glioma stem cells by mTORC1 activationm

Dissertation

Molecular mechanisms of metabolic regulation of glioma stem cells by mTORC1 activation

Mohamed Hegazy Mohamed Ahmed

Student ID No. 1323032003

Division of Life Science
Graduate School of Natural Science and Technology
Kanazawa University
JAPAN
2016

Table of Contents

Acknowledgement

First of all, I would like to express my deep thanks to my supervisor Professor. Atsushi Hirao for his support and advice during my PhD study at Kanazawa University. Without his help and encouragement, it would not have been possible to complete this research. Joining his research group was one of my best decisions I have made.

I would like also to thank all former and current laboratory members in Division of Molecular Genetics, Cancer and stem cells research program, Cancer Research institute, Kanazawa University, for their assistance and cooperation. Specially, Dr. Daisuke Yamada, Dr. Masahiko Kobayashi, Dr. Masaya Ueno, Dr. Mohamed A.E. Ali, Dr. Kumiko Ohta and Dr. Yuko Tadokoro.

Also, I would like to express my deep thanks for all collaborators from different laboratories, Prof. Chiaki Takahashi and Dr. Susumu Kohno form Division of Oncology and Molecular Biology, Cancer Research Institute, Kanazawa University. Prof.

Tomoki Todo and Dr. Yasushi Ino, Laboratory of Innovative Cancer Therapy, Institute of Medical Science, University of Tokyo. Prof. Tomoyoshi Soga, Institute for Advanced Biosciences, Keio University.

In addition, I would like to express my great thanks to Prof. Katsuji Yoshioka Division of Molecular Cell signaling, Cancer Research Institute, Kanazawa University for his academic support.

I am gratefully acknowledging financial support from the Egyptian Ministry of Higher Education and Mission Sector, whom made it possible for me to travel and study in Japan.

I would like to extend my thanks and appreciation to all my Professors at the Zoology Department, Faculty of Science, Minia University, Egypt, for their understanding, allowing me to get this opportunity to study abroad and obtaining a doctoral degree.

Finally, I also have much gratefulness to all my family members for getting me to this point.

List of Abbreviations

2-NBDG	2-N-7-nitrobenz-2-oxa-1,3-diazol-4-yl amino-2-deoxyglucose
3PGA	glycerophosphate, 3-phosphoglycerate
4-OHT	4-hydroxytamoxifen
4E-BP	4E-binding protein
6PGL	6-phosphogluconolactone
7AAD	7-Aminoactinomycin D
Abs	Antibodies
AKT	Protein kinase B (PKB)
AMPK	5' AMP-activated protein kinase
ATCC	American Type Culture Collection
BrdU	5-bromo-2'-deoxyuridine
BSA	Bovine serum albumin
CBP80	cap-binding protein 80
CDKN2A	Cyclin-Dependent Kinase Inhibitor 2A

CE-TOFMS	Capillary electrophoresis time-of-flight mass spectrometry
DAB	3,3′ -Diaminobenzidine
DMSO	Dimethyl sulfoxide
eEF2K	Eukaryotic translation elongation factor 2 kinase
EGF	Epidermal growth factor
EGFR	Epidermal growth factor receptor
eIF	Eukaryotic Initiation Factor
eIF4B	Eukaryotic translation initiation factor 4B
EMT	Epithelial- mesenchymal transition
EtOH	Ethanol
F1,6BP	Fructose 1,6-bisphosphate
FBS	Fetal bovine serum
FCCP	Carbonyl cyanide 4-(trifluoromethoxy)phenylhydrazone
FDA	US Food and Drug Administration
FGF2	Fibroblast Growth Factor 2

G6P	Glucose-6-phosphate
GAP	GTPase-Activating Protein
GBM	Glioblastoma
GFAP	Glial fibrillary acidic protein
GICs	Glioma initiating cells
Glut1	Glucose transporter 1
Grb10	Growth factor receptor-bound protein 10
Hk2	hexokinase2
huKO	humanized Kusabira-Orange
MDM2	Mouse double minute 2 homolog
mTORC1	Mammalian target of rapamycin complex 1
Nf1	Neurofibromin 1
NSPCs	Primary neural stem/progenitor cells
OCR	Oxygen consumption rate
p53	Tumor protein p53
p70S6K	p70 ribosomal protein S6 kinases

PBS	Phosphate-buffered saline
PDGFR	Platelet-derived growth factor receptor
PEP	Phosphoenol pyruvate
PGC1α	PPAR-γ coactivator 1α
PI3K	Phosphoinositide-3-kinase
PKM2	Pyruvate kinase isoenzyme type M2
PTEN	Phosphatase and tensin homolog
PVDF	Polyvinylidene difluoride
RB1	Retinoblastoma 1
ROS	Reactive oxygen species
RTK	Receptor tyrosine kinases
Ru5P	Ribulose-5-phosphate
S6	Ribosomal protein S6
S7P	Sedoheptulose 7-phosphate
SVZ	Subventricular zone
TAM	Tamoxifen

Tsc1	Tuberous Sclerosis 1
TuJ1	Neuron-specific class III beta-tubulin
Ulk1	Unc-51 Like Autophagy Activating Kinase 1
WHO	World Health Organization

Abstract

Although abnormal metabolic regulation is a critical determinant of cancer cell behavior, it is still unclear how an altered balance between ATP production and consumption contributes to malignancy. Here the results show that disruption of this energy balance efficiently suppresses aggressive malignant gliomas driven by mTOR complex 1 (mTORC1) hyperactivation. In a mouse glioma model, mTORC1 hyperactivation induced by conditional Tsc1 deletion increased numbers of glioma-initiating cells (GICs) *in vitro* and *in vivo*. Metabolic analysis revealed that mTORC1 hyperactivation enhanced mitochondrial biogenesis, as evidenced by elevations in oxygen consumption rate (OCR) and ATP production. Inhibition of mitochondrial ATP synthetase was more effective in repressing sphere formation by Tsc1-deficient glioma cells than that by Tsc1-competent glioma cells, indicating a crucial function for mitochondrial bioenergetic capacity in GIC expansion. To translate this observation into the development of novel therapeutics targeting malignant gliomas, I screened drug libraries for small molecule compounds showing greater efficacy in inhibiting the proliferation/survival

of Tsc1-deficient cells compared to controls. Several compounds able to preferentially inhibit mitochondrial activity, dramatically reducing ATP levels and blocking glioma sphere formation were identified. In human patient-derived glioma cells, nigericin, which reportedly suppresses cancer stem cell properties, induced AMPK phosphorylation that was associated with mTORC1 inactivation and induction of autophagy, and led to a marked decrease in sphere formation with loss of GIC marker expression. Furthermore, malignant characteristics of human glioma cells were markedly suppressed by nigericin treatment *in vivo*. Thus, targeting mTORC1-driven processes, particularly those involved in maintaining a cancer cell's energy balance, may be an effective therapeutic strategy for glioma patients.

Introduction

Metabolic regulation

Abnormal metabolic regulation is critical for malignant transformation leading to cancer(1,2). In particular, a tumor cell must maintain a proper energy balance between ATP production and its consumption to support the cell's heightened proliferation, survival and undifferentiated status. Historically, it has been believed that, even in the presence of oxygen, cancer cells generate energy mainly by glycolysis rather than through mitochondrial oxidative phosphorylation (OXYPHOS), a concept known as the Warburg effect(3). However, several previous studies using tumor cells lacking mitochondrial DNA challenged the Warburg hypothesis, because these data showed that tumors depend on mitochondrial respiration for the maintenance of fully transformed malignant phenotypes(4-7).

Metabolic regulation and Mitochondrial Activity

Recent studies demonstrated that mitochondrial activity is essential for malignant properties such as metastasis and multidrug resistance(8-10).

Accordingly, several small molecule compounds targeting mitochondrial function have been investigated for their anti-cancer effects(11). For example, numerous clinical studies of metformin, which inhibits mitochondrial complex I, have established the efficacy of this agent for cancer treatment. Other compounds that decrease mitochondrial bioenergetic capacity also have anti-tumor effects, therefore, targeting mitochondrial energetics is deemed to be a promising basis for new cancer therapies.

Mammalian target of rapamycin (mTOR)

The mammalian target of rapamycin (mTOR) is a serine/threonine protein kinase that belongs to the phosphoinositide-3-kinase (PI3K)-related protein kinase family. mTOR participates in two complexes, designated mTOR complex 1 (mTORC1) and 2 (mTORC2), both of which phosphorylate multiple substrates(12-14).

Both mTOR complexes are large; mTORC1 having six regulatory proteins, mammalian lethal with sec-13 protein 8 (mLST8, also known as GbL) with unknown role and even their loss doesn't affect mTORC1 activity to known substrates, (DEPTOR) or DEP domain containing mTOR-interacting protein

which is mTORC1 inhibitor, and the Tti1/Tel2 complex regulating the assembly and stability of mTORC1. Unlike mTORC2, mTORC1 have two specific regulatory proteins, regulatory-associated protein of mammalian target of rapamycin (raptor) which has an important role in the regulation of mTORC1 stability, localization and binding to substrates. Finally, proline-rich Akt substrate 40 kDa (PRAS40) a mTORC1 inhibitor (12).

However, mTORC2 have seven known regulatory protein components, three of them are unique to mTORC2, rapamycin-insensitive companion of mTOR (rictor) which is very important in regulation of the assembly and substrate binding to mTORC2, mammalian stress-activated map kinase-interacting protein 1 (mSin1) regulating the assembly and interaction of mTORC2 to SGK1 protein, and protein observed with rictor 1 and 2 (protor1/2) increases mTORC2 mediated activation of SGK1. The remaining regulatory components of mTORC2, like mTORC1 are mLST8, DEPTOR, Tti1 and Tel2 complex (12).

mTORC1 signaling

Activation of PI3K via receptor tyrosine kinases (RTKs) leads to activation

of AKT. AKT phosphorylates tuberous sclerosis complex (TSC) 2 and blocks the GAP activity of the TSC complex. The TSC complex exhibits GAP activity towards the small G protein Rheb and inhibits its ability, therefore, TSC complex is a negative regulator of mTORC1. Among mTORC1's substrates are the p70 ribosomal protein S6 kinases (p70S6Ks), eukaryotic Initiation Factor (eIF), 4E-binding proteins (4E-BPs), Ulk1, Lipin1, and Growth factor receptor-bound protein 10 (Grb10). Phosphorylation of 4E-BP1 by mTORC1 leads to its dissociation from eIF4E, allowing recruitment of eIF4G to the 5′ cap and translation initiation. p70S6Ks phosphorylate ribosomal protein S6, eukaryotic translation elongation factor 2 kinase (eEF2K), cap-binding protein 80 (CBP80), and eukaryotic translation initiation factor 4B (eIF4B), all of which stimulate protein synthesis (15,16).

mTOR signaling and Mitochondrial activity

On one hand, mTORC1 activation induces aerobic glycolysis by up-regulating pyruvate kinase isoenzyme type M2 (PKM2). On the other hand, mTORC1 activation stimulates several pathways that contribute to

mitochondrial activation and OXYPHOS. For example, mTORC1 is crucial for the mitochondrial activation mediated by PPAR-γ coactivator 1α (PGC1α) and the transcription factor Ying-Yang 1 (YY1)(15,16). Another study has demonstrated that mTORC1 stimulates the synthesis of nucleus-encoded mitochondrial proteins via 4E-BPs, resulting in increased mitochondrial ATP production(17). Since mRNA translation is the most energy-consuming process in the cell, mTORC1 coordinates both energy consumption and production, contributing to malignant progression.

Glioblastoma

Glioblastoma (GBM) is the most common high-grade malignant glioma in humans. GBM is categorized as a WHO grade IV astrocytoma, a very aggressive, invasive and destructive brain tumor (18). The major problem in glioma therapy is due to the infiltrative behavior of glioma cells and its ability to transfer into normal brain regions. Although the recent advances in the treatment of glioma, the number of patients diagnosed with glioma increase with a maximum survival of one year to one and half year. These recent methods in glioma therapies, like genetic screening of glioma tissues

or identification of signaling and molecular pathways involved in the development of glioma continues to have several challenges (19).

Glioma stem cells

Stem cells can be defined as the cells have the ability to self- renewal and differentiation into mature cells of a particular tissue. Stem cells are rare in most tissues. As a result, isolation of stem cells is very difficult and to study the biology and characteristics of stem cells, they must be isolated, purified and identified very carefully (20).

It is clear that normal stem cells and cancer sharing the self-renewal ability. There are many evidences show that cancer and normal stem cells sharing a lot of signaling pathways which is involved in regulation and development. From these pathways, the Notch signaling pathway, Sonic hedgehog pathway and Wnt signaling which are involved in oncogenesis in cancer tissues, these pathways may be involved also in the regulation of self-renewal of normal tissue stem cells (21).

The presence of cancer stem cells was first identified in the acute myeloid leukaemia (AML). In that study, the cell surface markers were used to

identify AML stem cells from the rest AML cells, which had a less proliferative capacity. More recent, the principle of cancer stem cells has been extended to different types of cancers such as, breast cancer and glioblastoma. The advances in research indicate that many types of tumor cells can be organized into hierarchies, containing malignant cancer stem cells, which have a high proliferative capacity, to more differentiated tumor cells, with a lower proliferative ability (22).

Numerous studies have identified a tumor cell population that can initiate glioma development. These cells are called glioma-initiating cells (GICs) and are conceptually recognized as "glioma stem cells"(23). It is the behavior of these GICs that determines the malignant phenotypes of GBM.

Genetic mutations in GBM

Alterations in several signaling cascades are known to affect gliomagenesis, including the RTK/RAS/PI3K pathway (EGFR, PDGFR, Nf1 and PTEN), the p53 pathway (TP53, CDKN2A/ARF and MDM2), and the RB pathway (RB1, CDKN2A/p16INK4A, CDKN2B and CDKN2C)(24). Consistent with the fact that activation of most of oncogenic signals triggers mTORC1

activation, the phosphorylation status of substrates of mTORC1 is a prognostic indicator for glioma patients(25-27).

mTORC1 signaling in GBM

Although the mTORC1 pathway is clearly a major player in gliomagenesis and malignant progression, mTORC1 inhibitors such as rapamycin and its analogs have failed to successfully treat GBM patients in the clinic. It is speculated that a feedback loop may exist in which mTOR inhibition by the allosteric inhibitors stimulates PI3K activation, supporting survival of tumor cells. Moreover, although mTOR ATP-competitive inhibitors and PI3K/mTOR inhibitors that fully inhibit substrate phosphorylation have been developed(28), these compounds are likely to have unwanted side-effects and may cause serious damage to normal tissues. Therefore, there is a pressing need to devise novel approaches to providing effective GBM therapy.

Aim of the present study

Previously, It has been reported that hyperactivation of mTORC1 in a murine inducible Tsc1 gene deletion resulted in early tumor onset in an EGFRvIII-driven mouse glioma model ($p16^{Ink4a}p19^{Arf}$ deficient background)(29). In that glioma model, Tsc1 deletion increased tumor mass and enhanced microvascular formation leading to intracranial hemorrhage, indicating that mTORC1 hyperactivation promotes malignant phenotypes of glioma *in vivo*. In the present study, first aim is to investigate the molecular mechanism by which mTORC1 hyperactivation causes the malignant phenotypes of glioma cells. Second aim is to identify small molecule compounds that may be effective for GBM therapy.

Materials and Methods

Mice

Rosa26-CreERT2 mice were the kind gift of Dr. Tyler Jacks (Massachusetts Institute of Technology). $p16^{Ink4a+/-}$ $p19^{Arf+/-}$ mice were obtained from the Mouse Models of Human Cancers Consortium of NCI-Frederick (30,31). $Tsc1^{f/f}$ mice were purchased from the Jackson Laboratory. For transplantation experiments using mouse and human glioma cells, BALB/c nu/nu mice (4-week-old females) were purchased from Sankyo Laboratory Service. All animal experiments were approved by the Committee on Animal Experimentation of Kanazawa University and performed following the University's Guidelines for the Care and Use of Laboratory Animals.

Mouse glioma model

Glioma-bearing mice were established as previously described(29). Briefly, primary neural stem/progenitor cells (NSPCs) were isolated from subventricular zone (SVZ) regions of $Tsc1^{f/f}$; Rosa26-$CreER^{T2}$ mice ($p16^{Ink4a-/-}p19^{Arf-/-}$ background) and cultured in Coaster Ultra-low attachment

plates (Corning) in serum-free NSPC medium, which contained DMEM/F12, B27 and 50 U/ml penicillin/ 0.5% streptomycin (all from Life Technologies), plus 20 ng/ml human FGF2 (Wako) and 20 ng/ml human EGF (Sigma). For preparation of retrovirus carrying EGFRvIII, Plat-E cells, provided by Dr. Toshio Kitamura (Institute of Medical Science, University of Tokyo), were transfected with pGCDN-EGFRvIII-IRES- humanized Kusabira-Orange (huKO), provided by Dr. Masafumi Onodera, National Research Institute for Child Health and Development (32). Retrovirus-containing supernatants were concentrated by centrifugation at 6,000xg for 16 hr. Cultured primary NSPCs were infected with pGCDN-EGFRvIII-IRES-huKO-expressing retroviruses for 24 hr and maintained in culture until transplantation. EGFRvIII-transduced NSPCs were dissociated into single cells, resuspended in 5% FBS/PBS, and $1x10^4$ cells were inoculated into the brains of anesthetized Balb/c nu/nu mice. For nigericin treatment *in vivo*, $1x10^6$ $huKO^+$ cells ($Tsc1^{f/f}$; Rosa-$CreER^{T2}$) were subcutaneously transplanted into female Balb/c nu/nu mice. To delete the Tsc1 gene in tumor cells *in vivo*, recipient mice were injected intraperitoneally (ip) with 1 mg/day tamoxifen (TAM, Sigma) or vehicle control (corn oil, Sigma) for 4 days. To isolate

glioma cells, tumor tissues were dissociated with the Brain Tumor Dissociation Kit (Miltenyi Biotec) and huKO^{+} cells were sorted using a BD FACSAria III instrument (BD). For transplantation of glioma cells, 100, 1,000 or 10,000 huKO^{+} cells were inoculated into the brains of recipient mice.

Cell culture

To delete the Tsc1 gene in mouse glioma cells *in vitro*, huKO^{+} cells (Tsc1$^{f/f}$; Rosa-CreER^{T2}) were cultured for 3 days in complete NSPC medium (containing EGF+FGF2) plus 0.1 μM 4-hydroxytamoxifen (4-OHT, Sigma). Cultures were washed clean of 4-OHT and cultured for another 2 days in complete NSPC medium. For sphere formation assays, single-cell suspensions were prepared using Accutase (Innovative Cell Technologies, Inc.) and filtered through a 40-μm cell strainer (BD), followed by culture for 7 days in NSPC medium with or without EGF+FGF2 and containing 1% methylcellulose (Wako). Human patient-derived GBM cells, termed TGS-01 and TGS-04, were established as described previously(33). Use of these human materials and protocols were approved by the Ethics Committees of Kanazawa University and the University of Tokyo. To increase pyruvic acid

level in glioma cells, sodium pyruvate stock solution (100 mM, Thermo Fisher Scientific) was added to normal NSPC medium (final concentration was increased from 0.5 to 1.5 mM).

CD133 Expression

To determine CD133 expression in the human glioma TGS-01 human patient-derived cells, TGS-01 cells treated with 0.5μM nigericin in adherent cell culture condition for 4 days. Next, cells were collected, centrifuged and filtered. Filtered cells were stained with anti-CD133 antibody (Ab) (Miltenyi Biotec #130-098-129), incubated on ice for 30 min, and analyzed by flow cytometry.

Drug screening

Libraries used for drug screening were: FDA-approved drug library (ENZO; CB-BML-2841J0100), ICCB known bioactives library (ENZO; CB-BML-2840J0100), kinase inhibitor library (ENZO; CB-BML-2832J0100), fatty acid library (ENZO; CB-BML-2803J0100) and phosphatase inhibitor library (ENZO; CB-BML-2834J0100). To confirm the effects of individual

compounds, we assayed nigericin (Sigma Aldrich), amoxapine (Wako), A23187 (Sigma Aldrich), valinomycin (Sigma Alderich), rottlerin (Abcam), auranofin (Abcam), clodronic acid (Cayman), moxifloxacin (Sigma Aldrich), nifidipine (Sigma Aldrich), minocycline (Santa Cruz Biotechnology), clindamycin (Sigma Aldrich) and pentamidine (Sigma Aldrich). Briefly, control and Tsc1-deficient glioma cells were treated with a compound at three doses (1/500, 1/2,000, and 1/10,000 dilution of provided compounds in the library) in 384-well plates (Corning) for 48 hr, followed by analysis of cell viability as mentioned below. The "Index for drug sensitivity of Tsc1-deficient glioma cells" was calculated as the ratio of value2/value1 at a specific dose of a compound, where value1 was for the drug efficacy in Tsc1-deficient glioma cells (e.g., 0.2 means 80% reduction), and value2 was for the drug efficacy in control cells (e.g., 0.8 means 20% reduction). An Index >1.0 means that Tsc1-deficient glioma cells were more sensitive than control glioma cells to the drug. An Index <1.0 means that loss of Tsc1 induced drug resistance.

Western blotting

Proteins were extracted with lysis buffer [0.1 M Tris (pH 6.7), 4% SDS, phosphatase inhibitor (Thermo Fisher Scientific), complete mini (Roche)] and quantified using a bicinchoninic acid (BCA) protein assay kit (Thermo Fisher Scientific). Proteins (5 μg) were fractionated by SDS-PAGE and transferred onto 0.45 mm polyvinylidene difluoride (PVDF) membranes (Millipore). Membranes were blocked in 5% (w/v) BSA/0.02% (v/v) Tween 20/PBS and incubated with primary antibodies (Abs) overnight at 4°C, followed by incubation with HRP-conjugated secondary Abs (GE Healthcare) and detection with ECL Prime (GE Healthcare). Primary Abs recognizing the following proteins were used: Tsc1 (#4906), pp70S6K (T389) (#9234), p70S6K (#2708), pS6(S235/236) (#4858), S6 (#2217), p4E-BP1 (T37/46) (#2855), 4E-BP1 (#9644), pAMPK alpha (T172) (#2535), AMPK alpha (#2532) (all from Cell Signaling Technologies, 1:1000), actin (Sigma-Aldrich #A5441, 1:2000), Nestin (Millipore #AB5922, 1:500), Olig2 (IBL #18953, 1:500), GFAP (BD #556328, 1:1000) , TuJ1 (Covance #MMS-435P,1:1000) and LC3 (NanoTools clone 5F10, #0231, 1:200).

PCR

Total RNA was extracted using the RNeasy Mini Kit (Qiagen). Total RNA was reverse-transcribed to cDNA using Super Script Reverse Transcriptase (Life technologies). Genomic and mitochondrial DNAs were extracted with 50 mM NaOH followed by neutralization with 1 M Tris-HCl. Real-time quantitative PCR was performed with Mx3000P (Stratagene). The following cycle parameters were used: denaturation at 95˚C for 30 sec, annealing for 30 sec at 58˚C, and elongation for 30 sec at 72˚C. Sequences of sense and antisense primers used were as follows:

Slc2a1 sense; 5`CAGTTCGGCTATAACACTGGTG3`, Slc2a1 antisense; 5`GCCCCCGACAGAGAAGATG3`, Hk2 sense; 5`TGATCGCCTGCTTATTCACGG3`, Hk2 antisense; 5`AACCGCCTAGAAATCTCCAGA3`, Pkm2 sense; 5`GCCGCCTGGACATTGACTC3` , Pkm2 antisense; 5`CCATGAGAGAAATTCAGCCGAG3`, Atp5g1 sense; 5`CCAGAGGCCCCATCTAAGC3`, Atp5g1 antisense; 5`CCCCAGAATGGCATAGGAGAAG3`, Cox5a1 sense;

5`GCCGCTGTCTGTTCCATTC3`, Cox5a1 antisense;

5`GCATCAATGTCTGGCTTGTTGAA3`, Cycs sense;

5`CCAAATCTCCACGGTCTGTTC3`, Cycs antisense;

5`ATCAGGGTATCCTCTCCCCAG3`, Actb sense;

5`GGCTGTATTCCCCTCCATCG3`, Actb antisense;

Intracellular ATP quantification

Intracellular ATP levels were quantified using the CellTiter-Glo Luminescent Cell Viability Assay (Promega) following the manufacturer's instructions. Briefly, cells were cultured in 96- or 384-well Ultra low attachment plates (Corning), and the luminescence representing the ATP level was measured by Infinite Pro 200 (Tecan).

Cell viability assay

Cell viability was assessed using the Cell Counting Kit-8 (Dojindo) following the manufacturer's instructions. Briefly, cells were incubated with WST-8 reagent for 3 hrs and absorbance at 450 nm was compared using Infinite Pro 200 (Tecan).

Quantification of metabolites

For capillary electrophoresis time-of-flight mass spectrometry (CE-TOFMS) analysis, three independent samples of control or Tsc1-deficient mouse glioma cells (3×10^6) that had been cultured in NSPC medium without EGF+FGF2 were lysed with methanol (1 ml) containing 25 μM internal standards (L- methionine sulfone, MES and CSA)(Wako), and homogenized to inactivate enzymes. The sample (400 μl) was transferred to a fresh tube, and 200 μl of chloroform was added. The mixture was centrifuged at 10,000 × g for 3 min at 4°C, and 400 μl of the upper aqueous layer was centrifugally filtered through a Millipore 5-kDa cutoff filter to remove proteins. The filtrate samples (320μl) were lyophilized and dissolved in 25 μl Milli-Q water containing 200 μM reference compounds (3-aminopyrrolidine, Adlrich, and trimesate, Wako) prior to CE-TOFMS analysis (34,35).

Mitochondrial membrane potential

To determine mitochondrial membrane potential, cells were treated for 30 min with small molecule compounds at the concentrations indicated in the Figure legends, followed by incubation with JC-10 dye buffer (Abcam) for

30 min at 37°C in 5% CO_2. Measurements of membrane potential were performed by flow cytometry.

Apoptosis

For Annexin V staining, TGS-01 human patient-derived glioma cells were treated with 1 μM nigericin for 6 hr, Then, cells incubated with PE-conjugated Annexin- V and 7AAD in Annexin V binding buffer (BD Biosciences) in accordance with the manufacturer's protocol. Measurements of Apoptosis were performed by flow cytometry.

Reactive oxygen species (ROS) generation

For analysis of mitochondria-derived ROS, cells were treated with 1 μM nigericin for 6 hr, incubated with 5 μM Mitosox Red (Life Technologies) for 30 min, washed twice with 5% FBS/PBS, and stained with 7AAD (BD Biosciences) to exclude dead cells. Measurements of ROS were performed by flow cytometry.

Oxygen consumption assay

The OCR was measured using an XF24 Extracellular Flux Analyzer (Seahorse Bioscience) according to manufacturer's protocol. For analysis of the effects of small molecule compounds on OCR, AGS cells (a human gastric cancer cell line, from ATCC) were seeded at $4x10^4$ cells/well in 500 μl supplemented culture medium (DMEM, Seahorse Bioscience #102365). OCR was measured at preset time intervals while the instrument automatically carried out preprogrammed additions of oligomycin (1 μM, Cell Signaling Technology #9996), FCCP (400 nM, Sigma #C2920) and antimycin A (1 μM, Sigma #A8674).

Cell cycle analysis

Cell cycle analysis was performed as previously described(36). Briefly, BrdU (10 μM) was added to the cultures and incubation continued at 37ºC for 30 min. Cells were collected and washed with PBS, followed by the addition of 70% EtOH (-30ºC) for 16 hr. Cells were then incubated with 2N HCl/0.5% Triton X-100 for 30 min at room temperature (RT), followed by treatment with 0.1 M borax buffer (10 mM borax, 50 mM boric acid) for 2

min at RT. Cells were stained with anti-BrdU-FITC Ab (BD Biosciences) for 1 hr at RT while avoiding light. Labeled cells were resuspended in PBS containing 1% bovine serum albumin and 7AAD (BD Biosciences), followed by cell cycle analysis by flow cytometry.

Tumor xenografts

Cells ($1x10^6$/100μl/inoculation site) were mixed with Matrigel Matrix (Fisher Scientific, Corning, NY, USA, no. 356234) (1:1.4 ratio) and subcutaneously transplanted into each of the two flanks of anesthetized female Balb/c nu/nu mice. Nigericin (4 mg/ml) or auranofin (12 mg/ml) dissolved in DMSO was mixed with corn oil (1:4 ratio). Nigericin (4 mg/kg/day, ip injection, every 2 days) or auranofin (12 mg/kg/day for 2 days, ip injection) was administered on day 1 after inoculation of TGS-01 cells. Tumor volume was measured using a conventional formula: volume (V) = $(W^2 \times L)/2$ where W=width and L=Length.

Immunohistochemistry

Tumors derived from xenografted patient-derived GBM cells were fixed with 4% paraformaldehyde at 4^oC overnight and embedded in paraffin.

Sections were stained with hematoxylin and eosin (HE). For immunostaining, sections were treated with Target Retrieval Solution (Dako), and stained with anti-Ki67 (BD#550609, 1:100), followed by visualization with a HRP-conjugated secondary Ab (GE Healthcare) and the DAB Peroxidase Substrate Kit (VECTOR). Stained sections were counterstained with hematoxylin and viewed using a microscope (Axio ImagerA1, Carl Zeiss).

Statistical analyses

Student's t test was used when comparing two groups, one-way (ANOVA) followed by Bonferroni's post hoc test when comparing more than two groups. For survival analysis in Fig.1C, differences in survival rate were analyzed by log-rank test. Calculations of significance were performed using Prism6 software: $*P < 0.05$, $**P < 0.01$, $***P < 0.001$, $****P < 0.0001$.

Results

mTORC1 hyperactivation expands mouse GICs *in vitro* and *in vivo*

To investigate the role of mTORC1 in GIC expansion, the previously described mouse glioma model in which mTORC1 is activated by a TAM-inducible system(29) was used. Briefly, NSPCs of $Tsc1^{f/f}$; $Rosa26\text{-}CreER^{T2}$ mice ($p16^{Ink4a-/-}$;$p19^{Arf-/-}$ background) were infected with retrovirus carrying EGFRvIII gene plus the huKO gene as a marker and injected these infected cells into the basal ganglia of immunocompromised mice. To activate mTORC1 in glioma tissue *in vivo*, TAM was administrated to NSPC-bearing recipient mice on day 5 post-transplantation. After gliomas had developed (at about 3 weeks post-transplantation), $huKO^{+}$ cells were collected from digested brain tissues of recipient mice and isolated glioma cells by flow cytometry. Efficient deletion of the *Tsc1* gene in this system has been previously confirmed by genomic DNA analysis(29).

To determine whether Tsc1 deficiency affected sphere formation, $huKO^{+}$ cells were cultured in ultra-low attachment dishes under standard NSPC culture conditions; that is, in the absence of serum but presence of the

growth factors, EGF and FGF2. Tsc1 deficiency significantly increased the number of spheres formed (**Fig.1**), indicating that the sphere-forming cells had expanded upon mTORC1 activation.

To evaluate the tumor-initiating capacity of glioma cells *in vivo*, recipient mice were inoculated with 100, 1,000 or 10,000 freshly isolated huKO^{+} glioma cells. It has been found that Tsc1 deficiency promoted tumor development and accelerated the death of recipients compared to Tsc1-competent glioma cells (**Fig.2**). When as few as 10 huKO^{+} cells were transplanted, only Tsc1-deficient glioma cells were capable of producing gliomas, but not control cells. Thus, GIC frequency is increased *in vivo* by mTORC1 activation.

mTORC1 activation causes growth factor-independent proliferation of mouse GICs

To investigate how mTORC1 activation affects the proliferation and survival of murine GICs, the effect of Tsc1 deletion on sphere formation *in vitro* was analyzed. Tsc1$^{f/f}$; Rosa26-CreER^{T2} glioma cells were allowed to form spheres in culture and then 4-OHT was added to delete the Tsc1 gene. First,

4-OHT efficiently induced Tsc1 deletion in these sphere cells was confirmed, as evidenced by the disappearance of Tsc1 protein from lysates of sphere cells that had been cultured with 4-OHT (**Fig.3**). However, unexpectedly, there was no difference in the number of spheres formed by control and Tsc1-deficient cells cultured in the presence of EGF+FGF2 **(Fig.4)**. This discrepancy may be due to differences between culture conditions *in vitro* and microenvironmental conditions *in vivo*. Although level of phosphorylation in 4E-BP1 was slightly up-regulated, those of S6 and p70S6K were almost normal in Tsc1-deficient glioma cells cultured under these conditions (**Fig.3**). It is speculated that, mTORC1 is fully activated when cytokines are abundant, and that levels of these factors are much higher *in vitro* than *in vivo,* therefore, Tsc1 deletion might not be able to further enhance such signaling in this culture condition. When control and Tsc1-deficient glioma cells were cultured in the absence of EGF+FGF2, the size and number of spheres formed in these control glioma cell cultures was decreased compared to those in control cultures containing growth factors, however, Tsc1-deficient glioma cells showed comparable sphere forming capacity in presence and absence of these growth factors (**Fig4**). Thus,

mTORC1 hyperactivation maintains sphere-forming capacity even when growth factors are withdrawn. Consistent with this observation, although levels of S6 and 4E-BP phosphorylation in control glioma cells cultured without growth factors were lower than those with growth factors, such down-regulation of phosphorylation due to growth factor depletion was not observed in Tsc1-deficient cells (**Fig.3**). Since the results did not show a remarkable change in the expression of Olig2, a glioma stem cell marker, in Tsc1-deficient glioma cells (**Fig.5**), which assume that Tsc1 deficiency promotes the proliferation and/or survival of GICs. Thus, mTORC1 hyperactivation induces GIC expansion that is independent of growth factors.

Increased sensitivity of Tsc1-deficient glioma cells to glucose depletion

Next the mechanism by which mTORC1 activation affects GIC growth in mouse glioma model was dissected. Although the metabolic status of whole glioma cells might not necessarily be identical to that of GICs due to tumor heterogeneity, metabolite levels were assessed in control and Tsc1-deficient glioma cells in culture *in vitro* using CE-TOFMS (34,35). Several metabolites in the glycolytic pathway, including glucose-6-phosphate (G6P),

fructose 1,6-bisphosphate (F1,6BP), glycerophosphate, 3-phosphoglycerate (3PGA), and phosphoenol pyruvate (PEP), were significantly up-regulated (Fig.6). The same was true for components of the pentose phosphate pathway, including 6-phosphogluconolactone (6PGL), ribulose-5-phosphate (Ru5P), and sedoheptulose 7-phosphate (S7P) (**Fig.6**). These findings suggested that glucose metabolism might be stimulated in Tsc1-deficient cells.

When gene expression levels were analyzed, Results showed that mRNAs encoding glycolytic enzymes such as glucose transporter 1 (Glut1), hexokinase2 (Hk2), and pyruvate kinase M2 (PKM2) were all elevated by mTORC1 activation (**Fig.7**). These data indicate that mouse glioma cells experiencing mTORC1 hyperactivation show increased dependence on glucose.

Enhanced mitochondrial ATP production supports mTORC1-driven GIC expansion

Metabolomics analysis showed that lactate levels in glioma cells were not significantly affected by Tsc1 deletion (**Fig.6**). These data suggested that the increased glucose uptake exhibited by Tsc1-deficient cells might contribute

to enhanced mitochondrial OXPHOS rather than to the production of lactate via typical glycolysis. To determine OXPHOS in these cells, OCR was evaluated and found that it was significantly increased in Tsc1-deficient glioma cells (**Fig.8**). In addition, the expression levels of mitochondria-associated genes were up-regulated by Tsc1 deletion (**Fig.9**). Consistent with this enhanced mitochondrial activity, ATP levels were increased in Tsc1-deficient cells compared to controls (**Fig.10, left**). To assess whether this increase in ATP in Tsc1-deficient cells was in fact due to enhanced OXPHOS, the cells were treated with oligomycin, an ATP synthetase inhibitor. Interestingly, while oligomycin had only a modest effect on ATP levels in control cells, it dramatically reduced ATP levels in Tsc1-deficient cells (**Fig.10, right**).

Consistent with the marked ATP reduction in oligomycin-treated Tsc1-deficient glioma cells, oligomycin also profoundly suppressed sphere formation by Tsc1-deficient cells compared to controls (**Fig.11**). These results indicate that mTORC1 hyperactivation stimulates mitochondrial ATP production that is vital for the vigorous expansion of GICs.

Drug screening to identify small molecule compounds that can suppress sphere formation by Tsc1-deficient mouse glioma cells

The new application of a known drug, called drug repositioning or drug repurposing, has been a beneficial approach for developing novel therapies for human diseases. With this in mind, I assessed whether this mouse glioma model would be useful for drug screening to identify known compounds able to specifically inhibit the aggressive phenotypes of glioma cells. To this end, I evaluated the effects of numerous small molecule compounds from commercially available existing drug libraries (a total of 1,301 compounds) on the proliferation/survival of control and Tsc1-deficient mouse glioma cells. To compare the efficacy of an individual compound on control vs. Tsc1-deficient cells, First the inhibitory effect was estimated for each compound on both types of cells, and then the ratio of the inhibitory effect on Tsc1-deficient cells compared to its effect on control cells was calculated; this ratio was termed the "Index for drug sensitivity of Tsc1-deficient cells" (see Experimental Procedures).

Most compounds screened exhibited an Index of about 1.0 ± 0.5 (**Fig.12**), indicating that they had equal effects on control and Tsc1-deficient

cells. Several compounds showed low Index values, suggesting that these drugs were less effective in inhibiting the growth of Tsc1-deficient cells than that of control cells. For example, I found that the EGFR inhibitors gefitinib and erlotinib showed less efficacy in Tsc1-deficient cells than in control cells (**Fig.13)**. Several genotoxic reagents, including mitoxantrone and topotecan, were also less efficacious in Tsc1-deficient cells (**Fig.14**), suggesting that mTORC1 hyperactivation allows glioma cells to resist conventional chemotherapy. In contrast to the above, several compounds were identified that were highly effective in inhibiting the growth of Tsc1-deficient glioma cells compared to that of control cells **(Fig.15)**.

From the first screening, 13 drugs were selected (nigericin, amoxapine, A23187, auranofin, rottlerin, valinomycin, minocycline, nifedipine, pentamidine, cyclosporine, clodronic acid, clindamycin and moxifloxacin) that showed reproducible increased efficacy in Tsc1-deficient cells compared to controls. The concentrations of these compounds used in this screening was approximately 0.5-30 μM.

Next, I screened the selected compounds for those that caused a greater reduction in intracellular ATP levels in Tsc1-deficient cells, based on

the previous observation that oligomycin treatment triggered a significant reduction in ATP in the former. I found that 5 drugs (nigericin, A23187, auranofin, rottlerin and valinomycin) clearly reduced intracellular ATP levels when used at less than 20 μM (**Fig.16**). Most of these drugs showed greater inhibitory effects on Tsc1-deficient cells than on control cells, although there were differences in efficacy among these compounds. I confirmed that these 5 compounds also had a greater suppressive effect on sphere formation by Tsc1-dificent glioma cells than on that by control cells (**Fig.17**), suggesting that the screening system could efficiently identify drug candidates in therapeutic approach for mTORC1-driven glioma.

To investigate whether the selected compounds could affect the behavior of human GBM cells as well as mouse Tsc1-deficient glioma cells, I applied each agent to human patient-derived GBM cell lines (TGS-01 and TSG-04 cells). Although it is unclear exactly which GBM sub-type these cells represent, they appear to have characteristics similar to the proneural type (rather than to the mesenchymal type) because they express relatively high levels of CD133, which is a proneural sub-type marker(37). A recent proteomics analysis has demonstrated that, compared to mesenchymal

GBMs, proneural GBMs show elevated expression and activation of elements of the PI3K-AKT-mTORC1 pathway(24). Therefore, like the Tsc1-deficient mouse glioma cells used in this study, human TGS-01 and TSG-04 GBM cells may exhibit relatively high levels of mTORC1. I found that all the 5 drug compounds reduced ATP in TGS-01 cells compared to untreated GBM cells (**Fig.18**).

All compounds also induced abnormality in mitochondrial membrane potential (**Fig.19**). Nigericin (a K^+/H^+ ion exchanger) induced mitochondrial membrane hyperpolarization, as previously reported(38), whereas A23187 (Ca^{2+} ionophore), rottlerin (K^+ ionophore) and valinomycin (K^+ ionophore) triggered depolarization (**Fig.19**), indicating that an abnormality of ion channels causes mitochondrial dysfunction. Cells exposed to auranofin, a gold (I)-phosphine derivative used to treat rheumatoid arthritis, also showed depolarization, because this agent reportedly induces the mitochondrial membrane permeability transition, which is manifested as mitochondrial swelling and loss of membrane potential(39). This means that treatment with most of these selected compounds might drive down intracellular ATP levels by interfering with

mitochondrial ATP production.

Since it was previously reported that nigericin and valinomycin affect mitochondrial respiratory chain (40), Conferment of their effects was performed. After downregulation of OCR by ATP synthase inhibition (oligomycin treatment), it was recovered by valinomycin (as expected), because valinomycin is an uncoupler (**Fig.20**). In contrast, nigericin treatment blocked the respiratory chain and maintained its suppression even after addition of FCCP (an uncoupler), indicating that nigericin is an efficient inhibitor of mitochondrial bioenergetics. Thus, compounds selected by a combination of the "Index for drug sensitivity in Tsc1-deficient mouse glioma cells" and their effects on ATP levels induce mitochondrial dysfunction. These data demonstrate that the drug screening system used in this study can efficiently select small molecule compounds capable of disrupting a glioma cell's energy balance.

Nigericin suppresses malignant phenotypes of human patient-derived GBM cells

Next I investigated whether the selected compounds might have therapeutic

potential for human GBM. Among the candidates, nigericin has previously been selected by a drug screening program as being capable of targeting cancer stem cell properties, which are induced by the epithelial-mesenchymal transition (EMT). Therefore, I focused on nigericin to determine if this compound could have advantage in suppression of malignant phenotypes of human GBM cells *in vitro* and *in vivo*. I found that nigericin could indeed effectively reduce sphere formation by human GBM cells in culture (**Fig.21**). While nigericin treatment blocked the cell cycle, specifically S-phase entry as determined by BrdU incorporation (**Fig.22**), it did not induce significant apoptosis (**Fig.23**). Mitochondrial ROS were up-regulated in glioma cells as detected by MitoSOX (**Fig.24**), indicating that nigericin induces mitochondrial dysfunction. Moreover, expression levels of the glioma stem cell markers, Olig2 and CD133, were dramatically downregulated during culture with nigericin (**Fig.25, 26**). These data indicate that nigericin suppresses proliferation of GBM cells, associated with the loss of stem cell properties. Interestingly, nigericin clearly triggered AMPK phosphorylation that was associated with marked inhibition of phosphorylated S6K and 4EBP1 (**Fig.27**), suggesting that downregulation of

ATP levels stimulates an anti-tumor signaling cascade that includes AMPK activation and mTORC1 inactivation. mTOR inhibition and AMPK activation are both known to induce autophagy(12), and, as expected, nigericin dramatically induced autophagy in glioma cells as determined by an observed increase in the LC3-II/LC3-I ratio **(Fig.27)**.

To investigate whether nigericin inhibits sphere formation due to abnormality in energy control, concentration of sodium pyruvate was increased in culture media, because pyruvic acid supplies energy to cells through the OXYPHOS in the presence of oxygen. As a result, addition of sodium pyruvate mitigated the inhibitory effect of low concentration, but not higher concentration (>0.1 μM), of nigericin on sphere formation (**Fig.28**). These data suggest that low dose of nigericin inhibits sphere formation due to partial, but not complete, impairment of mitochondrial energy production. Although remarkable changes of energy signals were not observed with such low dose of nigericin, presumably due to subtle changes below detectable limits, these data support an idea that energy imbalance causes dysfunction of GICs.

Lastly, I determined whether nigericin administration could inhibit

glioma growth *in vivo*. Immunocompromised mice were injected with human GBM cells and tumor development was monitored. Indeed, tumor volume (**Fig.29)** was greatly reduced in nigericin-treated recipient mice. Histological analyses showed that important histological hallmarks for GBM malignancy, such as remarkable vasculature formation and pseudopalisading necrosis, were observed in control tumor tissues. In contrast, these malignant characteristics dramatically disappeared by nigericin treatment *in vivo* (**Fig.30**). Also, results showed down-regulation of Ki67 staining, by nigericin treatment *in vivo* (**Fig.31**). When the effect of nigericin on tumor cell growth in recipient mice bearing $Tsc1^{\Delta/\Delta}$ or control mouse glioma cells were evaluated, I found that nigericin profoundly suppressed the growth of Tsc1-deficient tumors *in vivo*, consistent with *in vitro* results (**Fig.32).**

In addition, when I evaluated the effects of other candidate agents auranofin, A23187, Rottlerin and valinomycin on human GBM cells, I found that all of these compounds suppressed sphere formation on both human patient derived glioma cell lines TGS-01 and TGS-04 (**Fig.33,34**). Then, auranofin was selected to perform an *in vivo* experiment because this agent has been clinically approved for treatment of rheumatoid disease as

mentioned above. auranofin treatment of glioma-bearing mice resulted in a significant reduction in GBM growth *in vivo* (**Fig.35**). Like nigericin, Histological analyses after auranofin treatment showed a remarkable reduction in vasculature formation and pseudopalisading necrosis which observed in control tumor tissues, but not in auranofin treated tissues **(Fig. 36)**. Immunohistochemical analysis showed a clear reduction in the proliferation as evidenced by the proliferation marker ki67 after auranofin treatment *in vivo* **(Fig.37)**.

These data clearly indicate that this screening system based on an mTORC1-driven glioma model is useful for selecting compounds able to target aggressive malignant gliomas.

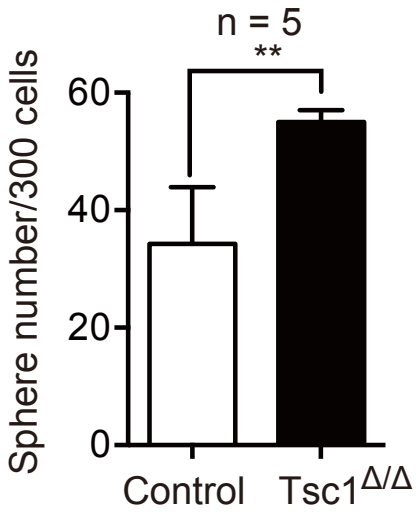

Figure 1. Sphere formation assay in control and Tsc1 deficient cells. Quantitation of sphere formation by huKO^{+} cells isolated from recipient mice that had been treated with (Tsc1$^{\Delta/\Delta}$) or without (control) TAM to delet*e* *Tsc1*. Data are the mean sphere number ± SD.

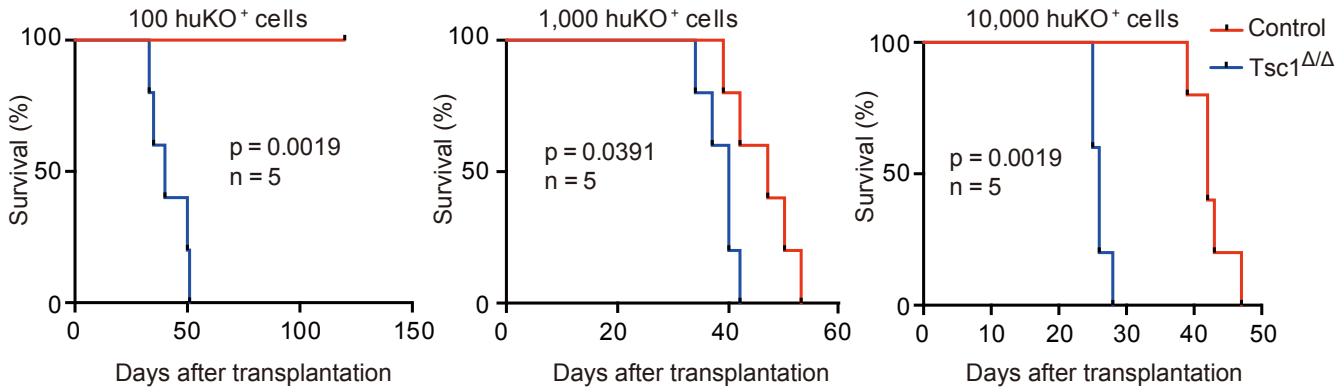

Figure 2. Tsc1 deletion leads to GIC expansion in vivo. Kaplan-Meier analysis of survival of recipient mice inoculated with 100, 1,000 or 10,000 huKO^{+} cells that had been treated with (Tsc1$^{\Delta/\Delta}$) or without (control) TAM.

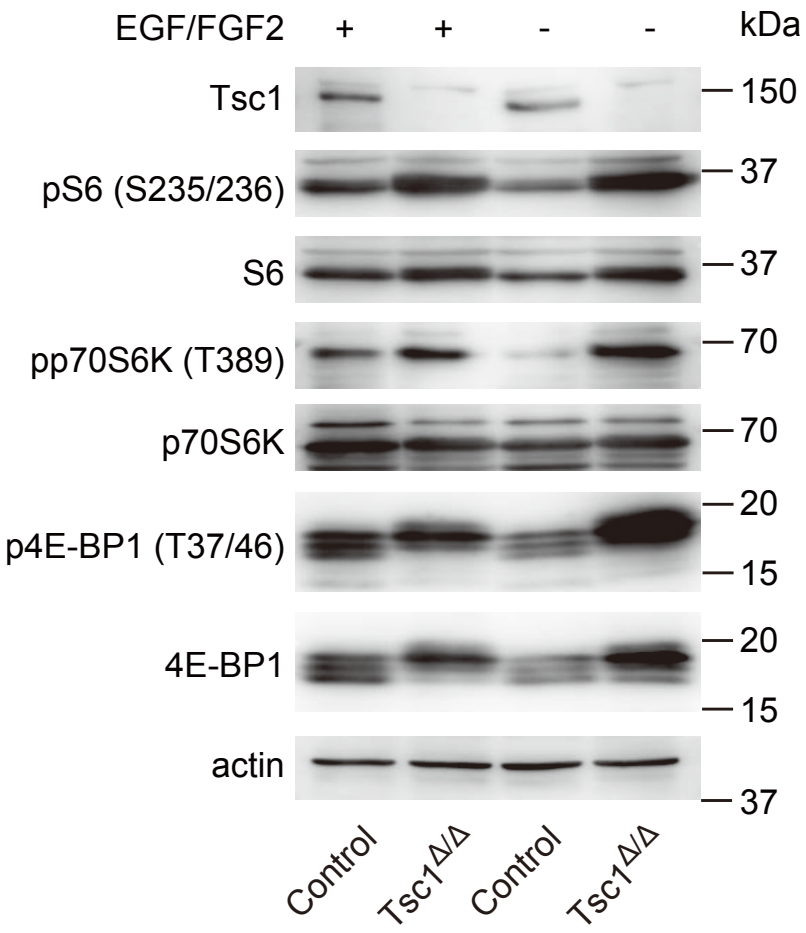

Figure 3. Tsc1 deletion and mTORC1 pathway. Western blot to detect the indicated proteins in control and $Tsc1^{\Delta/\Delta}$ cells. Deletion of *Tsc1* gene *in vitro* was induced with 4-OHT treatment to prepare $Tsc1^{\Delta/\Delta}$ cells (see Experimental Procedures). Lysates were prepared from control and $Tsc1^{\Delta/\Delta}$ cells treated with/without EGF+FGF2 for 24 hr. Actin, loading control.

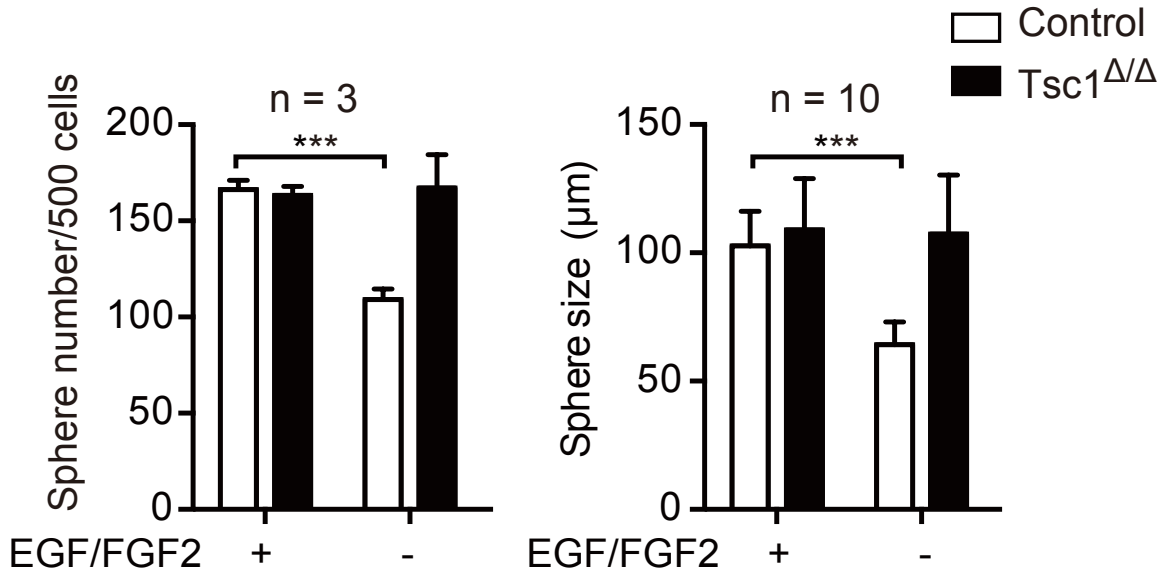

Figure 4. Expansion of GICs induced by Tsc1 deletion is independent of growth factors. Quantitation of sphere formation of control and $Tsc1^{\Delta/\Delta}$ cells cultured with/without EGF+FGF2. Data are the mean sphere number (left panel) and size (right panel) ± SD.

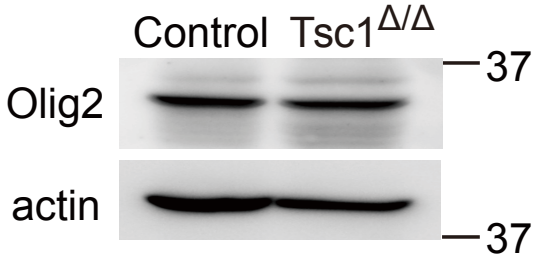

Figure 5. Olig2 expression in control and Tsc1 deleted mouse glioma cells. Western blot to detect Olig2 in control and $Tsc1^{\Delta/\Delta}$ cells cultured without EGF+FGF2 for 5 days.

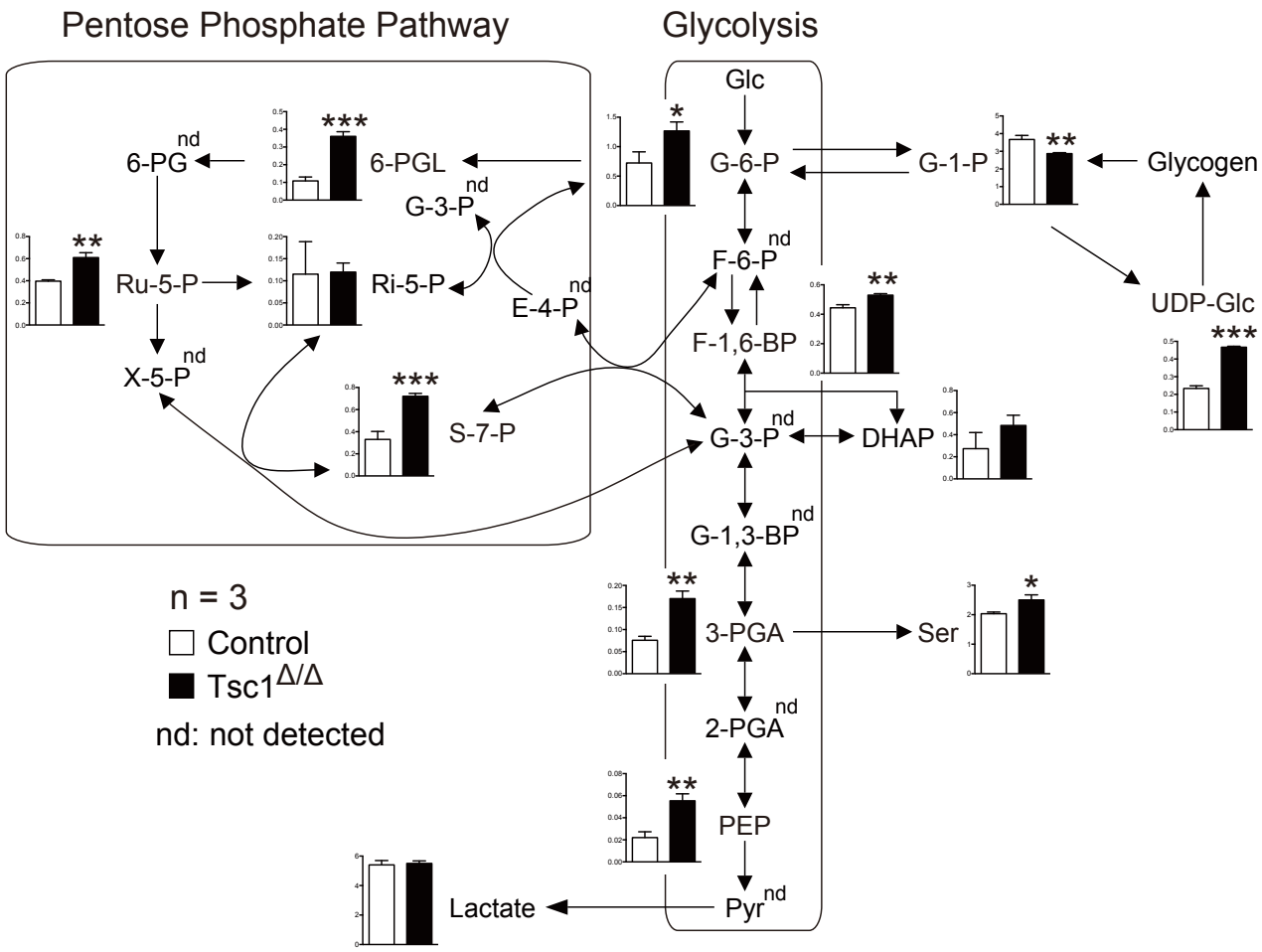

Figure 6. Metabolomics Analysis. Scheme showing quantitation of changes to metabolites in the pentose phosphate and glycolysis pathways that were associated with Tsc1 deletion in huKO^{+} cells. Control and Tsc1-deficient cells were cultured without EGF+FGF2 and subjected to quantification of metabolites. Data for each metabolite are the mean ratio ± SD relative to the value in control cells.

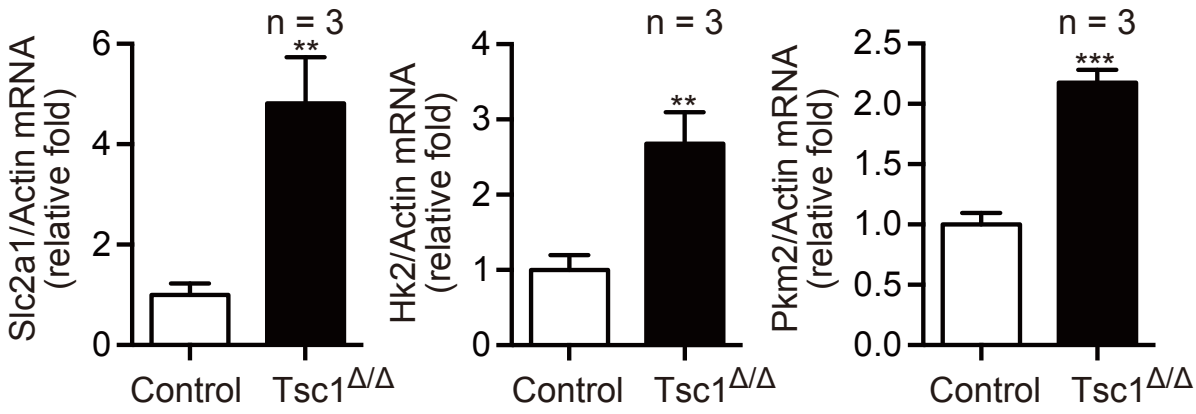

Figure 7. Gene expression analysis of Glycolysis associated genes. qRT-PCR analysis of Glut1, Hk2, and Pkm2 mRNA levels in the control and Tsc1-deficient cells. Data were normalized to β-actin and are presented as the mean fold change ± SD relative to control cells.

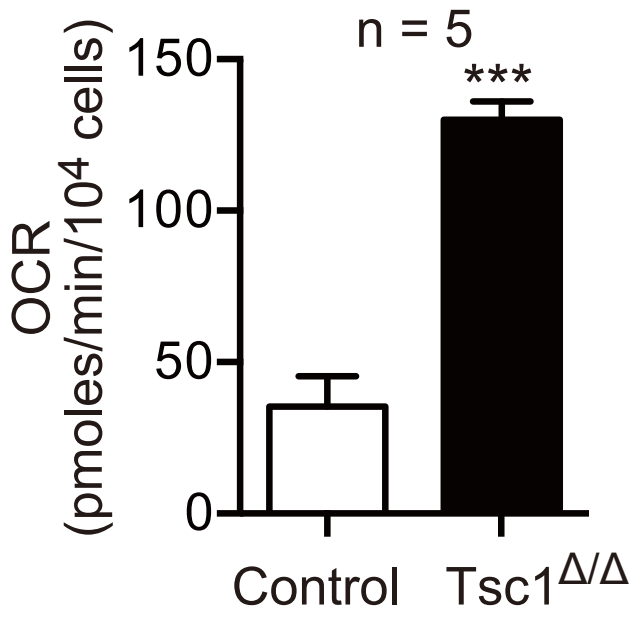

Figure 8. Effects of Tsc1 deficiency on oxygen consumption in mouse glioma cells. Quantitation of OCR by control and Tsc1-deficient cells cultured without EGF+FGF2. Data are the mean ± SD.

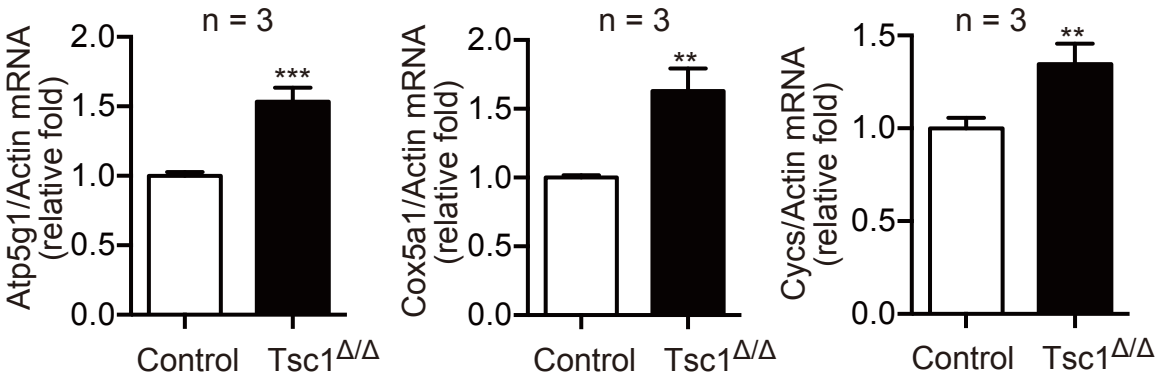

Figure 9. Mitochondrial associated genes levels in control and Tsc1 deficient mouse glioma cells. qRT-PCR analysis of Atp5g1, Cox5a1, and cytochrome c mRNA levels. Data are the mean fold change ± SD relative to control cells.

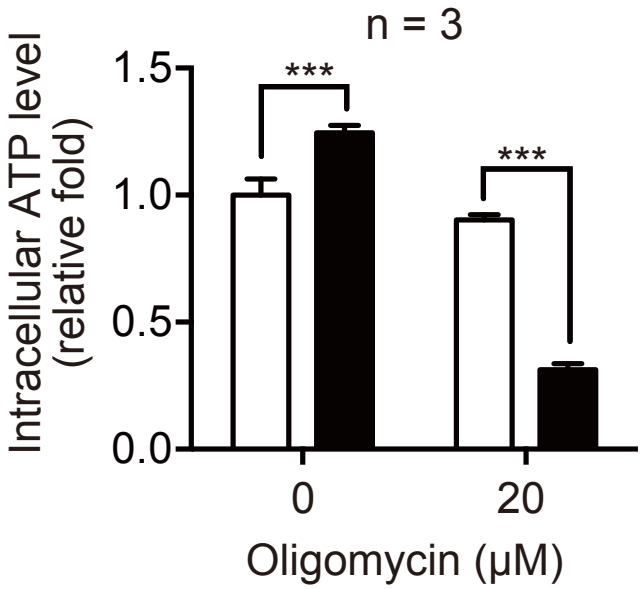

Figure 10. Effects of Oligomycin treatment ATP levels in control and Tsc1 deficient mouse glioma cells. Quantitation of intracellular ATP levels in control and Tsc1-deficient cells that were cultured without EGF+FGF2 and treated with the ATP synthetase inhibitor oligomycin for 12 hr. Data are the mean fold change ± SD relative to control cells.

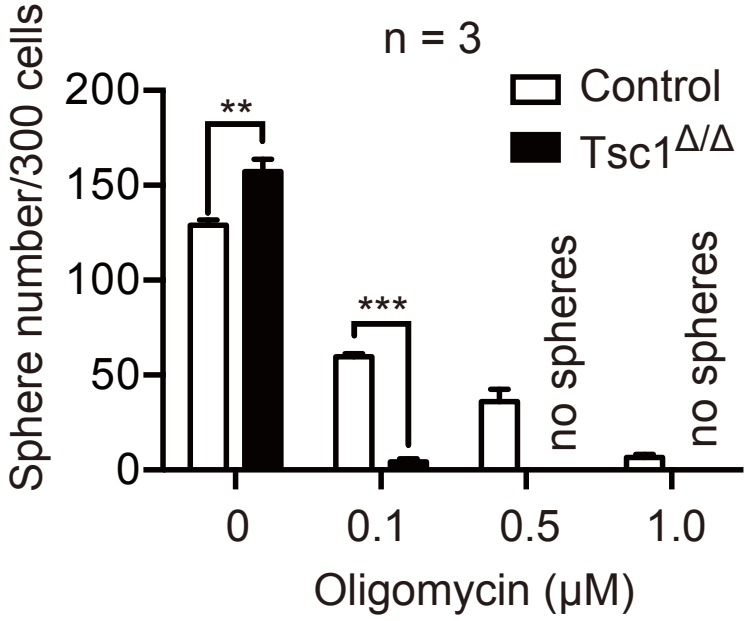

Figure 11. Effects of Tsc1 deficiency and Oligomycin treatment on sphere formation in mouse glioma cells. Quantitation of sphere formation by control and Tsc1-deficient cells that were cultured without EGF+FGF2 and treated with the indicated concentrations of oligomycin. Data are the mean ± SD.

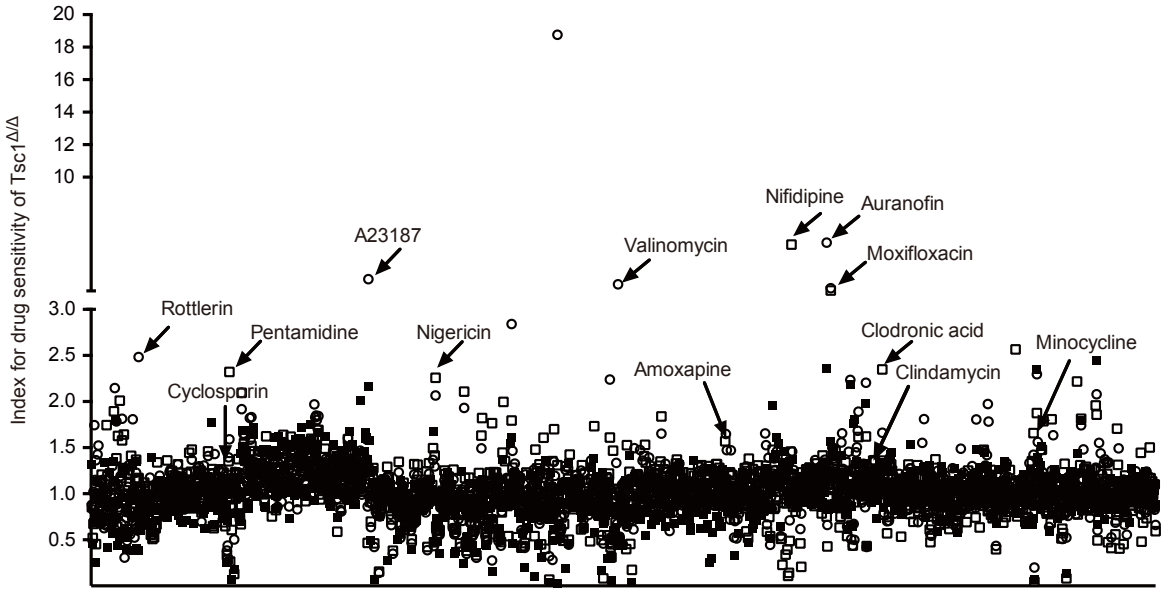

Figure 12. Drug screening for small molecule compounds that have a greater growth inhibitory effect on Tsc1-deficient glioma cells than on control cells. The "Index for drug sensitivity of Tsc1-deficient glioma cells" (see Experimental Procedures) for 1,301 compounds is shown. Control and Tsc1-deficient cells were treated with the indicated small molecule compounds, followed by analysis of cell viability 48 hr later (□ ;1/500, ○ ;1/2,000 or ■ ;1/10,000 dilution).

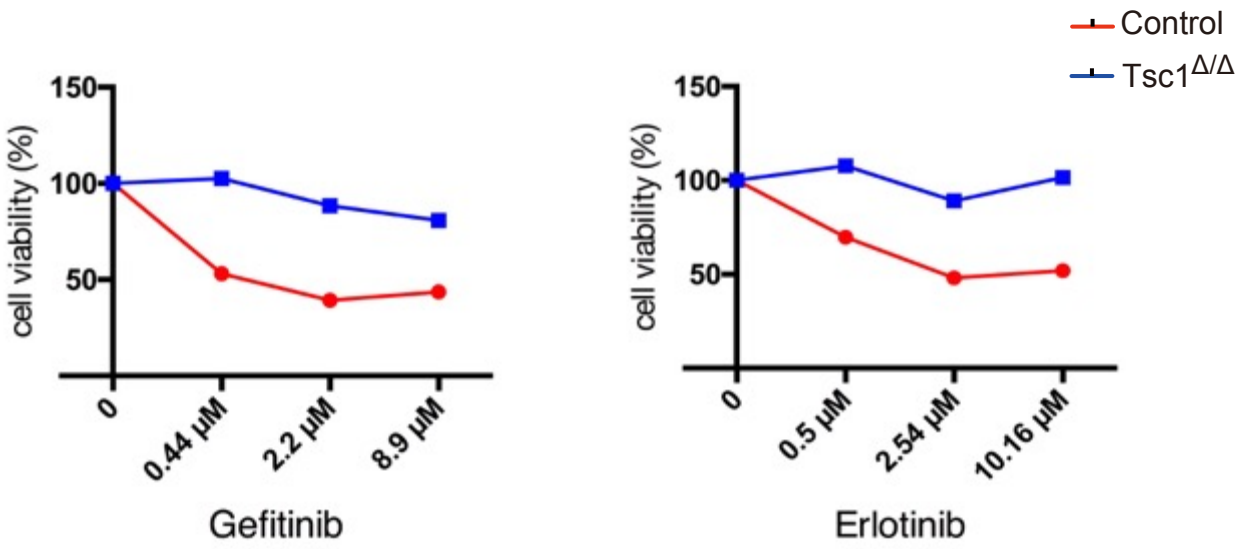

Figure 13. Examples of EGFR "drug-resistant" profiles. Quantitation of relative viability of control or Tsc1-deficient cells that were cultured without EGF+FGF2 and treated with the indicated concentrations of the indicated drugs. Data are expressed as the mean % cell viability relative to untreated controls.

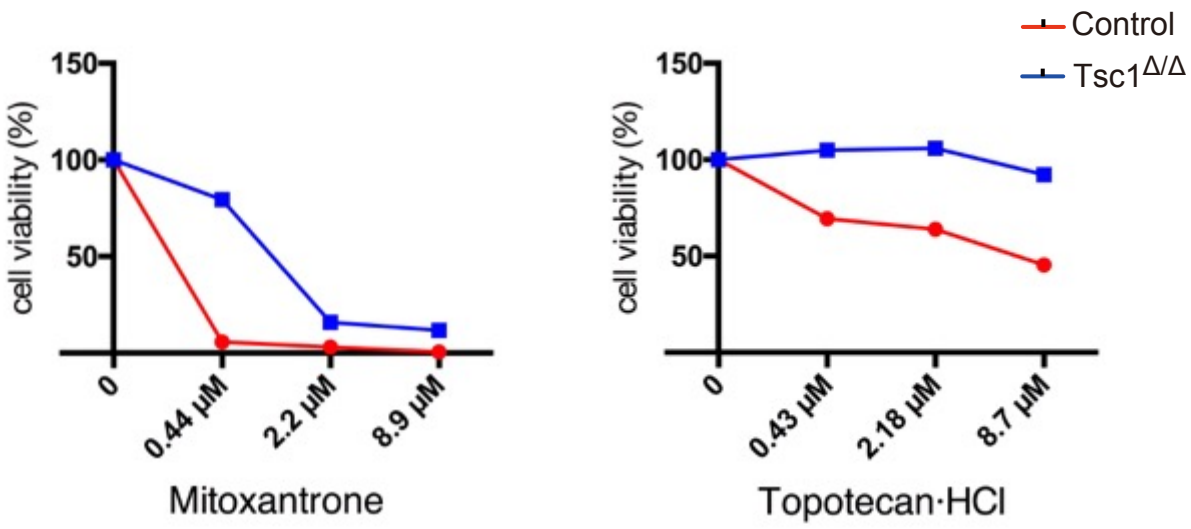

Figure 14. Examples of Genotoxic agents "drug-resistant" profiles. Quantitation of relative viability of control or Tsc1-deficient cells that were cultured without EGF+FGF2 and treated with the indicated concentrations of the indicated drugs. Data are expressed as the mean % cell viability relative to untreated controls.

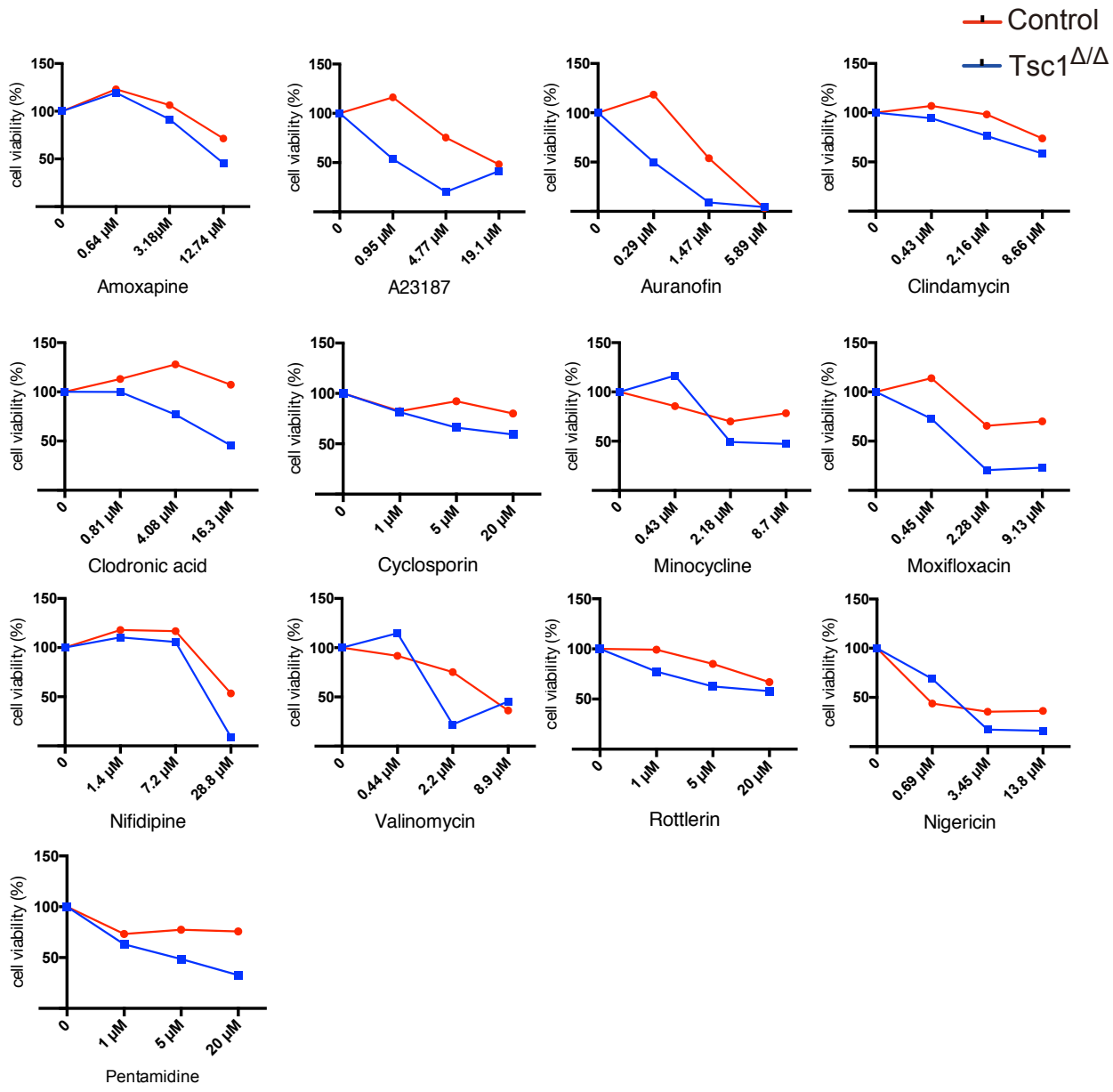

Figure 15. Examples of "drug-sensitive" profiles. Quantitation of relative viability of control or Tsc1-deficient cells that were cultured without EGF+FGF2 and treated with the indicated concentrations of the indicated drugs. Data are expressed as the mean % cell viability relative to untreated controls.

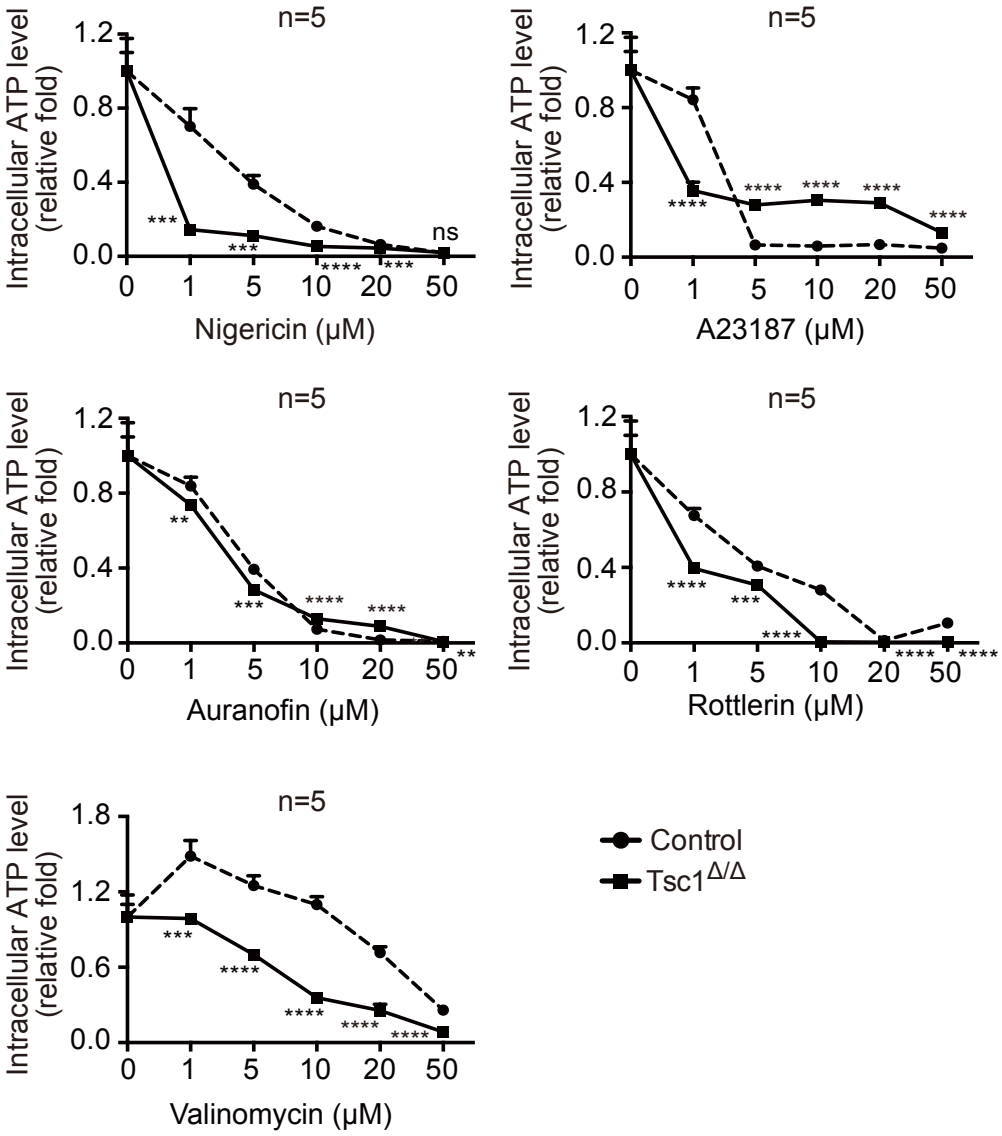

Figure 16. Effect of selected small molecule compounds on ATP levels of mouse glioma cells. Quantitation of the effects of the indicated small molecule compounds on ATP levels in control and Tsc1-deficient cells that were treated with the indicated compounds at the indicated concentrations. Cells were treated for (6 hr) was followed by analysis of intracellular ATP levels. Data are the mean ratios ± SD relative to untreated control cells. Statistical analyses were performed to detect differences between control and Tsc1-deficient cells at each drug concentration.

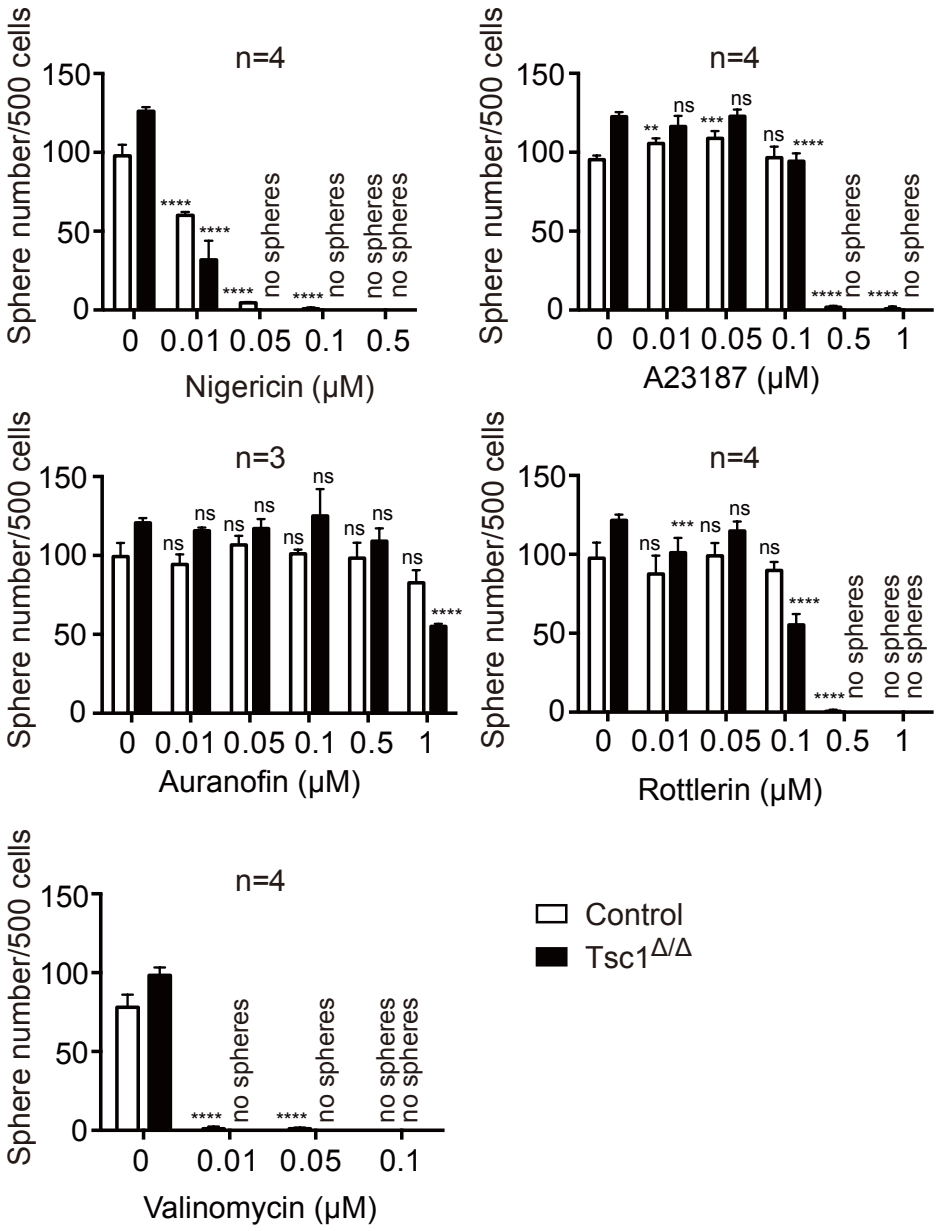

Figure 17. Effect of selected small molecule compounds on sphere-forming ability of control and Tsc1-deficient glioma cells. Quantitation of the effects of the indicated small molecule compounds on sphere formation in control and Tsc1-deficient cells that were treated with the indicated compounds at the indicated concentrations. cells were cultured to allow sphere formation. Data are the mean sphere number ± SD. Statistical analyses were performed to detect differences between treated and untreated cells at each drug concentration.

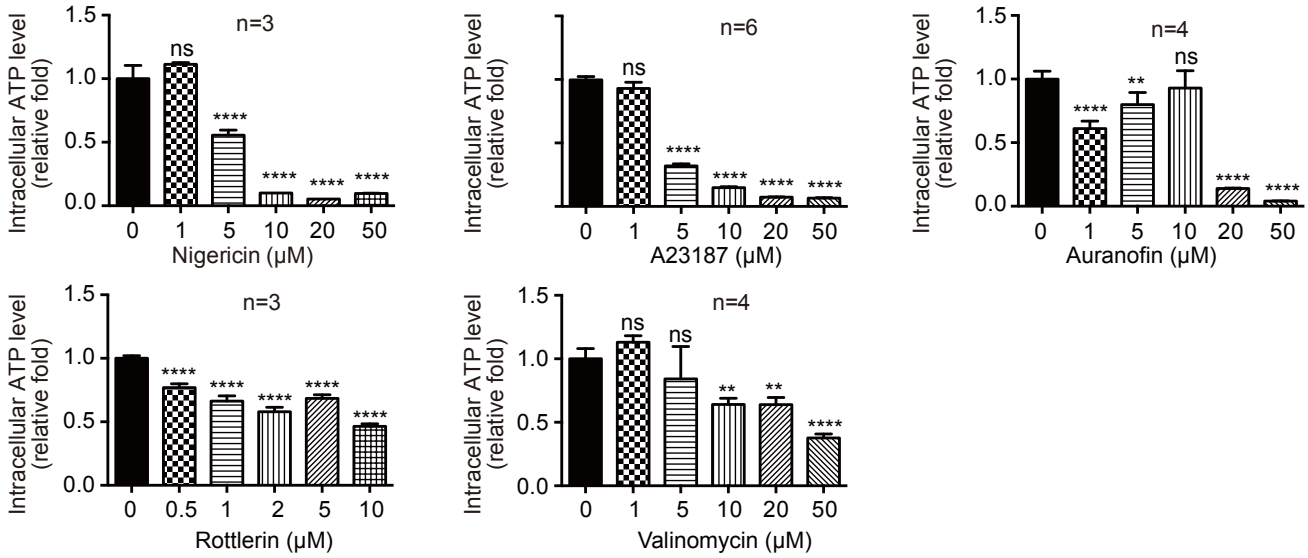

Figure 18. Effects of selected small molecule compounds on ATP levels on human patient-derived TGS-01 glioma cells. Quantitation of intracellular ATP levels in human GBM patient-derived TGS-01 cells that were treated with the indicated concentrations of the indicated compounds for 6 hr. Data are the mean fold change ± SD relative to untreated control cells.

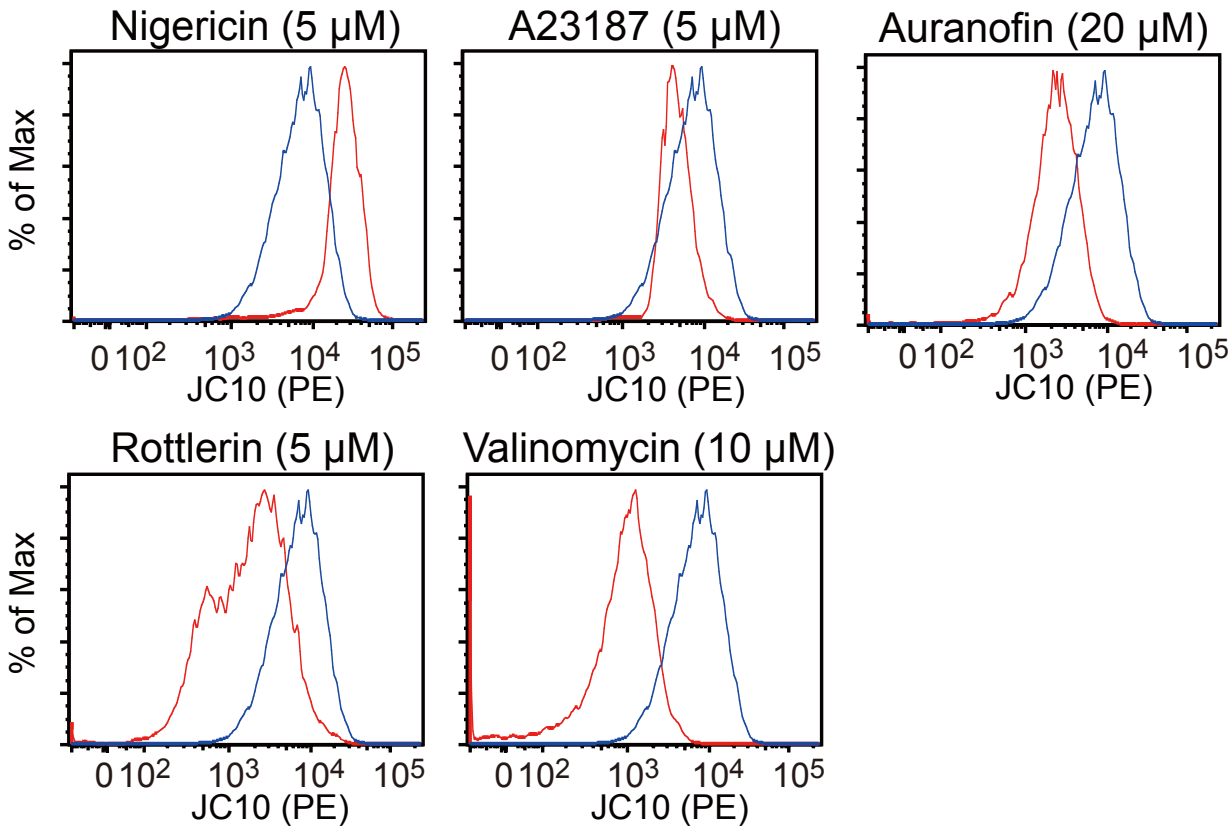

Figure 19. Effects of selected small molecule compounds on mitochondrial membrane potential on TGS-01 human patient derived glioma cells. Analysis of mitochondrial membrane potential in TGS-01 cells that were treated for 30 min with the indicated concentrations of the indicated compounds, followed by determination of mitochondrial membrane potential using JC-10. Representative flow cytometric data for cells with (red line) or without (blue line) drug treatment are shown.

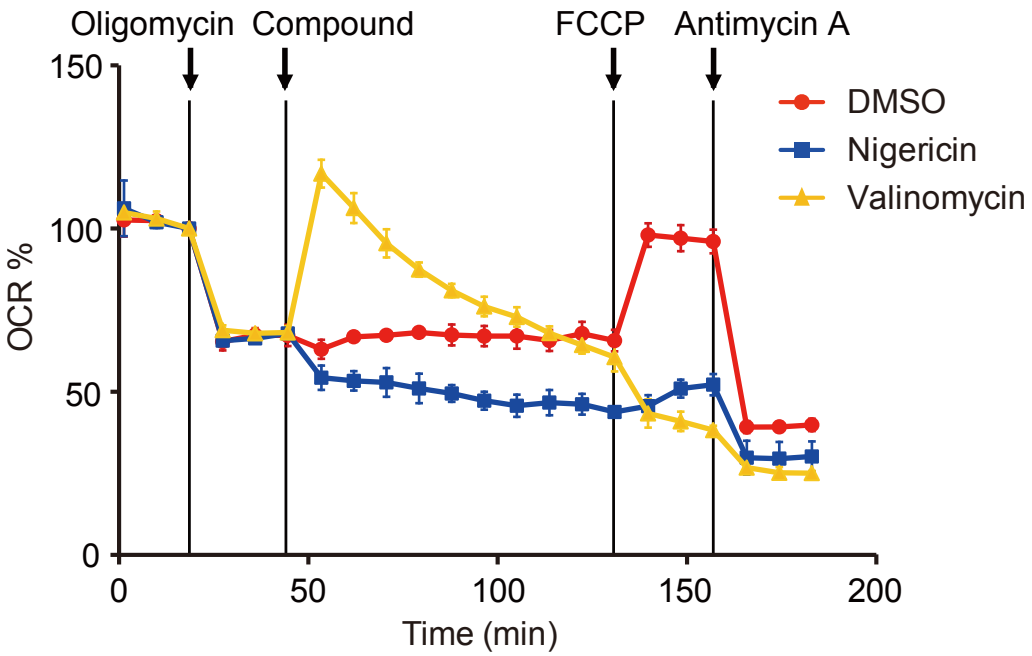

Figure 20. Effects of selected small molecule compounds on oxygen consumption rate. Quantitation of changes in OCR in AGS cells that were treated first with oligomycin to inhibit ATP synthetase activity and then with DMSO (vehicle control), nigericin (1 μM) or valinomycin (1 μM) (n=3). Data are mean %± SD of OCR (n=3).

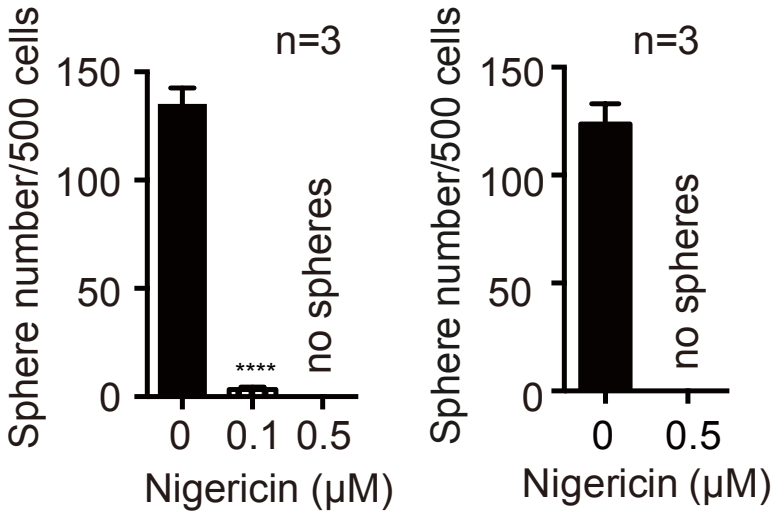

Figure 21. Therapeutic potential of nigericin for treatment of human GBM *in vitro*. Quantitation of sphere formation by (left) TGS-01 and (right) TGS-04 human patient-derived GBM cells that were treated with the indicated concentrations of nigericin. Data are the mean sphere number ± SD.

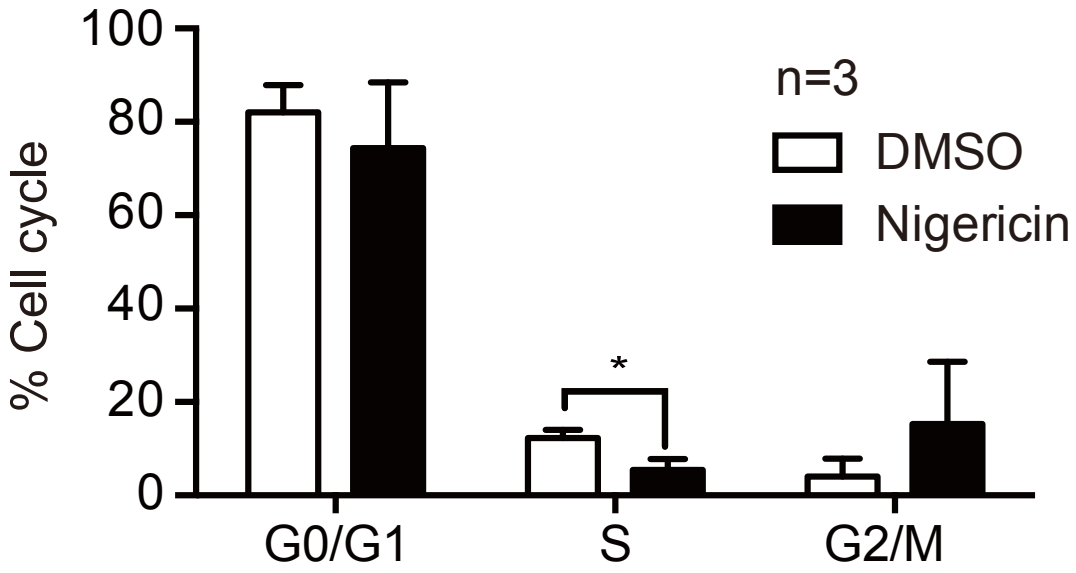

Figure 22. Cell cycle analysis after Nigericin treatment in TGS-01 human glioma cells. Cell cycle analysis of TGS-01 cells that were treated with 5 μM nigericin for 3 hrs. Data are the mean percentage of cells ± SD in the indicated stages of the cell cycle.

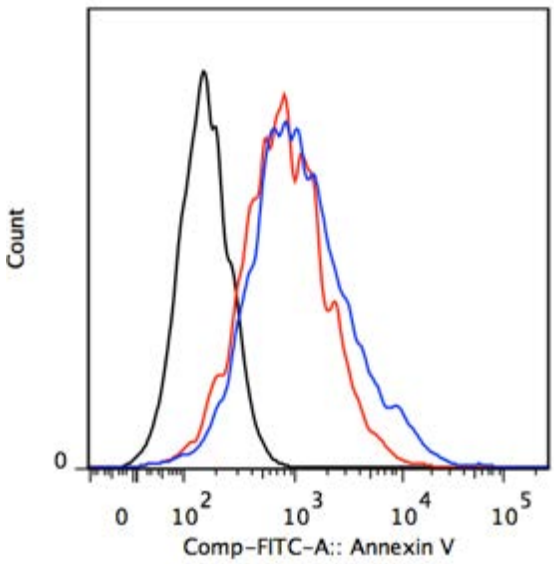

Figure 23. Effect of Nigericin treatment on Apoptosis on TGS-01. Representative Annexin V flow cytometric analysis in TGS-01 cells that were treated with 1 μM nigericin for 6 hr. Black, no staining; blue, DMSO control; red, nigericin.

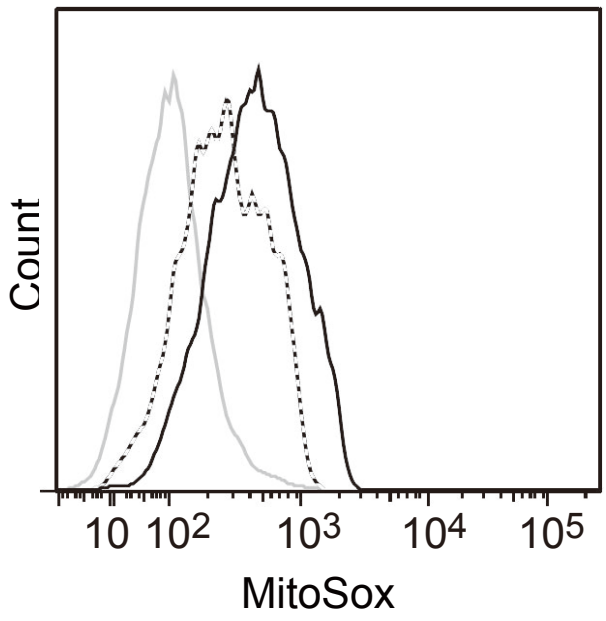

Figure 24. Effect of Nigericin treatment on Mitochondrial ROS generation on TGS-01. Representative MitoSOX flow cytometric analysis of mitochondrial ROS in TGS-01 cells that were treated with 1 μM nigericin for 6 hr. Gray line, no staining; black dashed, DMSO control; black solid, nigericin.

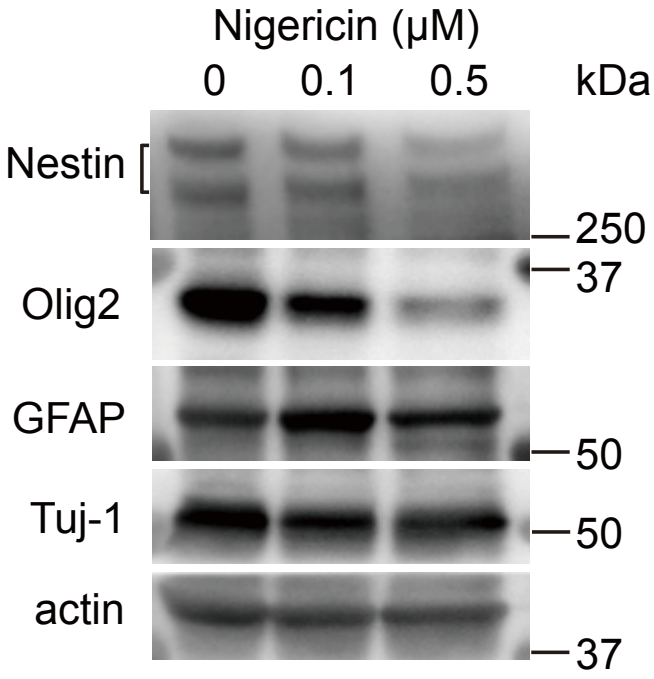

Figure 25. Glioma stem cells markers expression. Expression of GIC markers of TGS-01 cells that treated with 0.1 or 0.5μM nigericin in adherent cell culture condition for 4 days. Western blot to detect the indicated proteins.

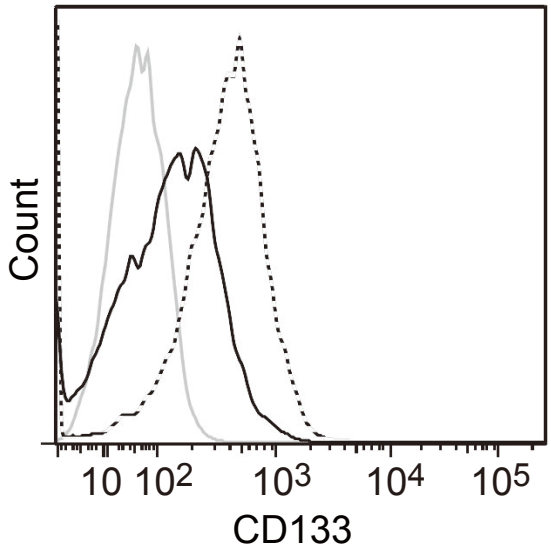

Figure 26. Expression of CD133 in TGS-01 cells that treated with 0.5μM nigericin in adherent cell culture condition for 4 days. Representative flow cytometric analysis of CD133 expression. Gray line, no staining; black dashed, DMSO control; black solid, nigericin.

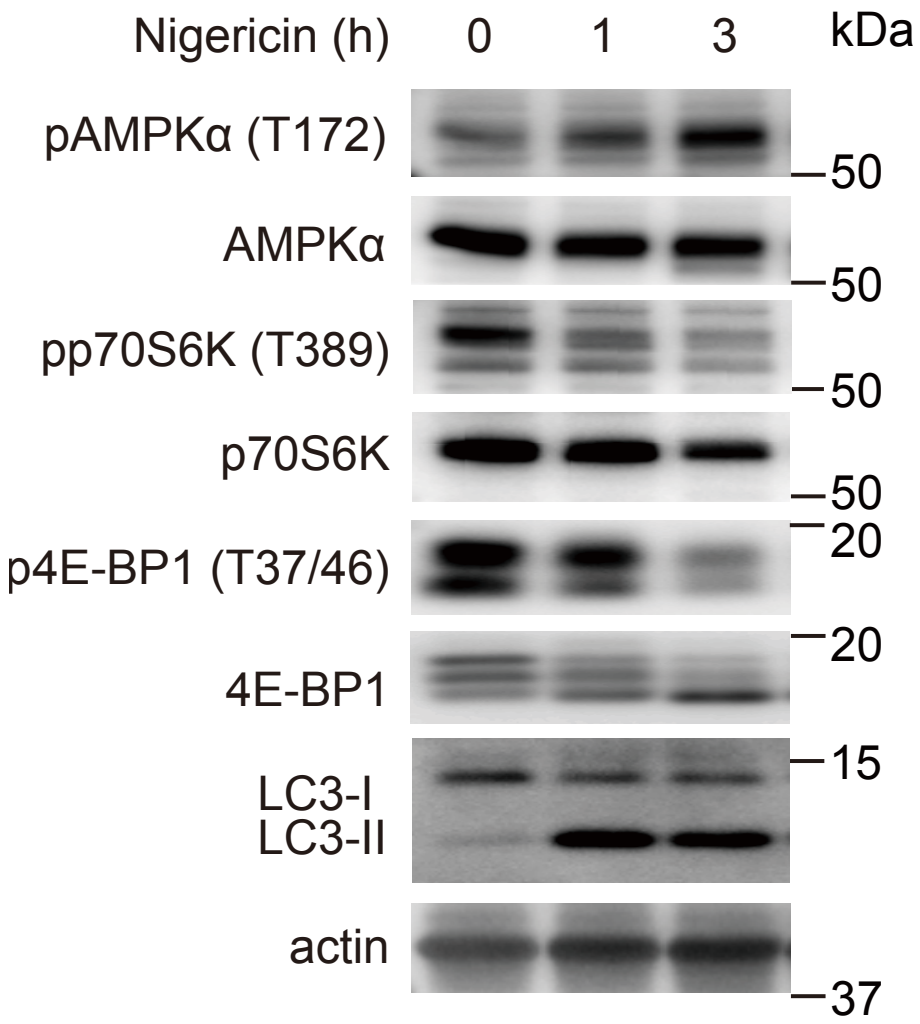

Figure 27. AMPK expression, Autophagy and mTORC1 signaling after treatment with Nigericin. Western blot to detect the indicated proteins in TGS-01 cells that treated with 5 μM nigericin for 0, 1 or 3 hr.

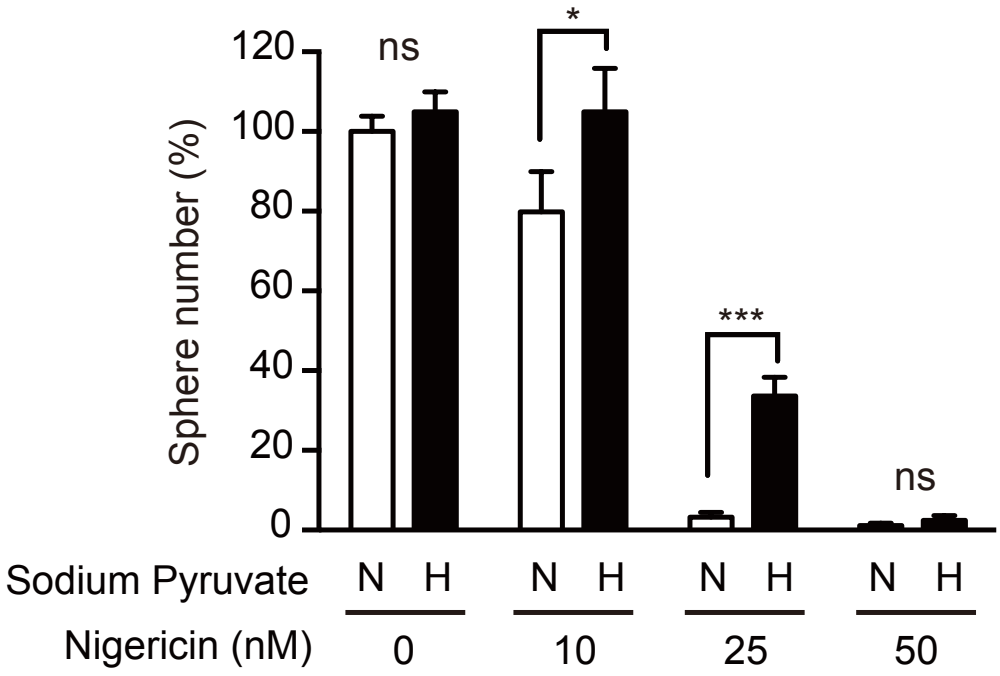

Figure 28. Sphere formation ability after Nigericin treatment and Pyruvate addition. Quantitation of sphere formation by TGS-01 cells that were treated with nigericin in culture media containing normal (0.5 mM) or high concentration (1.5 mM) of sodium pyruvate. N, normal concentration; H, high concentration. Data are the mean ratios of sphere number ± SD relative to untreated cells with normal concentration of sodium pyruvate.

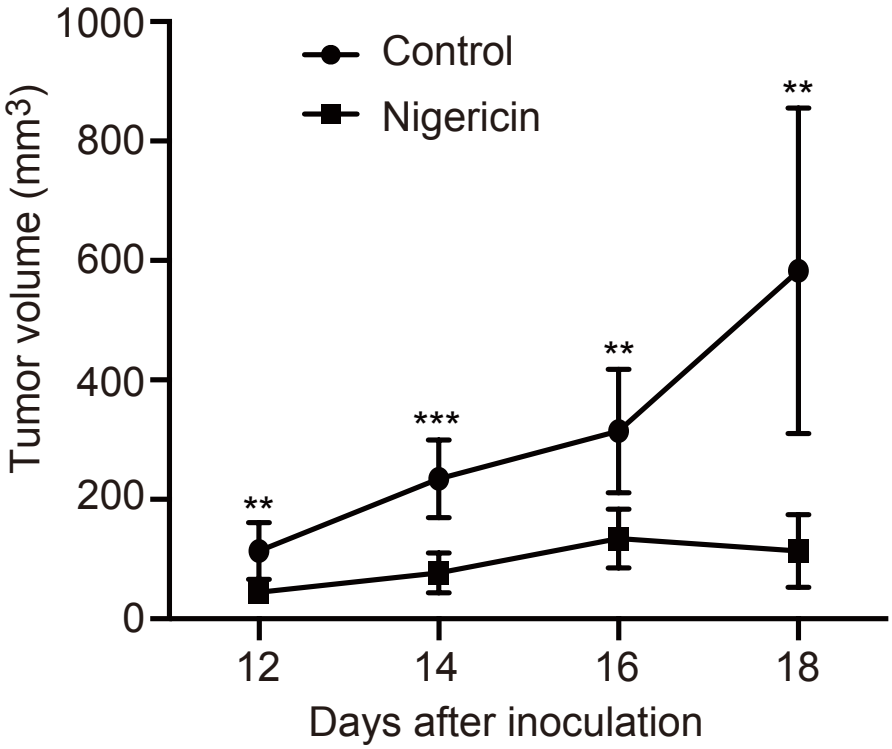

Figure 29. Therapeutic potential of nigericin for treatment of human GBM *in vivo*. Quantitation of volumes of tumors in mice that had been subcutaneously inoculated with TGS-01 cells and treated with DMSO (control) or nigericin. Data are the mean volume ± SD for tumors from control (n=6) and nigericin-treated (n=8) mice. Statistical analyses were performed to detect differences between treated and untreated mice.

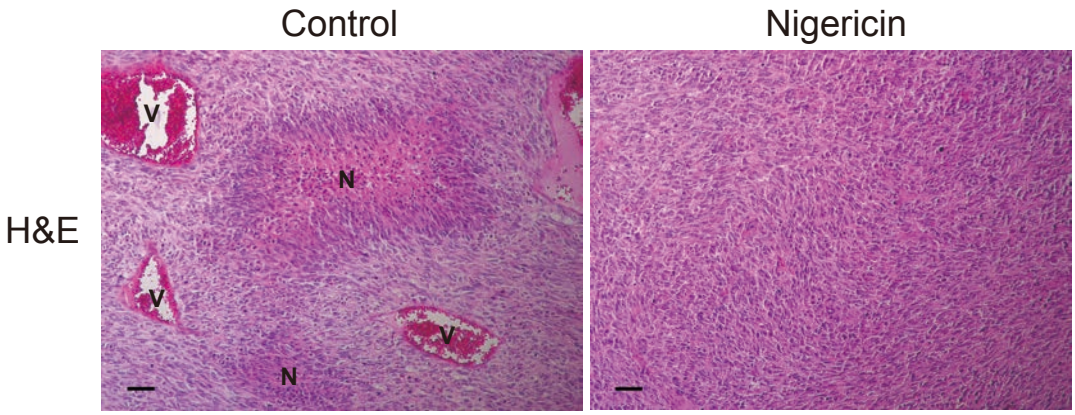

Figure 30. Immunohistochemical analysis of tumor sections after Nigericin treatment. Immunohistochemistry analyses of tumors that were isolated from the mice in (Fig.29) and subjected to HE staining. Data are representative of 6 tumors examined/group. Scale bars, 50 μm. V and N indicate vasculature and necrotic area, respectively.

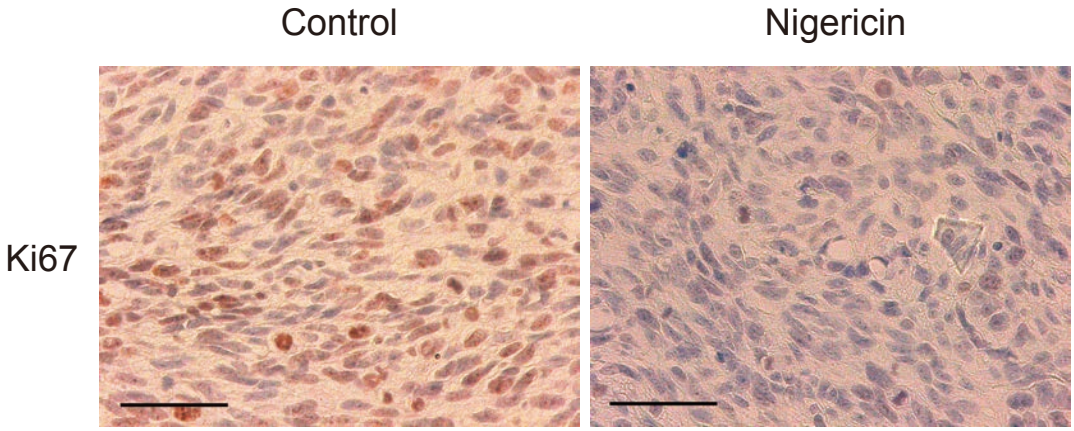

Figure 31. Immunohistochemical analysis of tumor sections after Nigericin treatment. Immunohistochemistry analyses of tumors that were isolated from the mice in (Fig.29) and subjected to immunostaining with Ki67 antibody. Data are representative of 6 tumors examined/group. Scale bars, 50 μm.

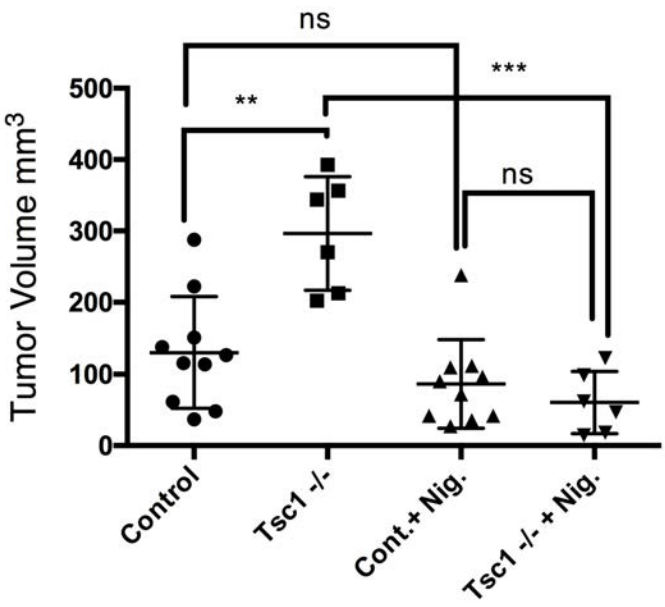

Figure 32. Therapeutic potential of nigericin for treatment of mouse GBM *in vivo.* Quantitation of volumes of tumors in mice subcutaneously inoculated with huKO^{+} glioma cells (Tsc1$^{f/f}$;Rosa-CreER^{T2}) and treated with/without TAM, which was administrated on day 1 after tumor cell inoculation. Nigericin (4 mg/kg/day, ip injection, every 2 days) was administered on day 6 post-inoculation. Data are the mean volume ± SD for tumors from control (n=10) and nigericin-treated (n=6) mice at 16 days after tumor cell inoculation.

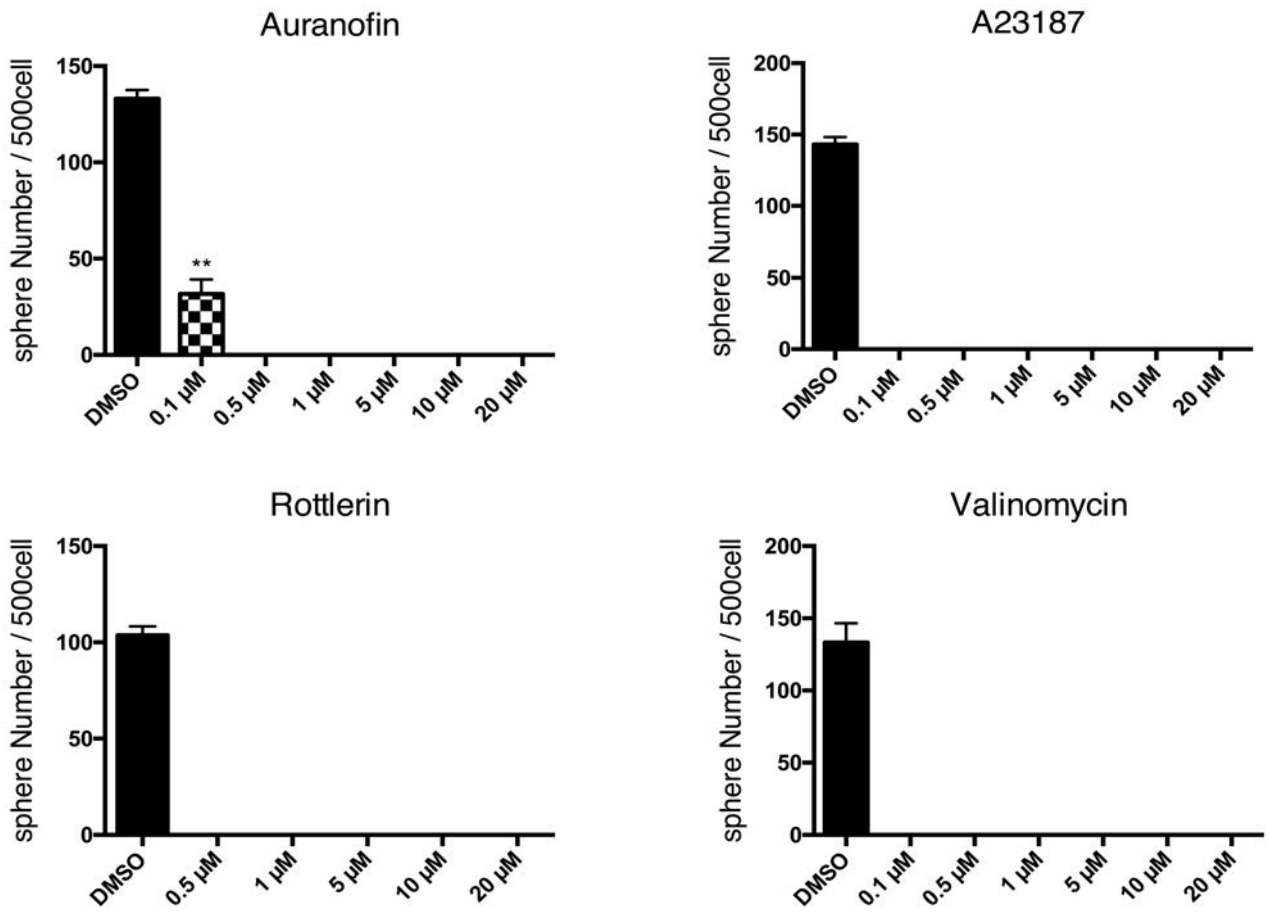

Figure 33. Therapeutic potential of other compounds for treatment of human GBM *in vitro*. Quantitation of sphere formation in TGS-01 human patient-derived GBM cells that were treated with the indicated concentrations of compounds. Data are the mean sphere number ± SD. n=3

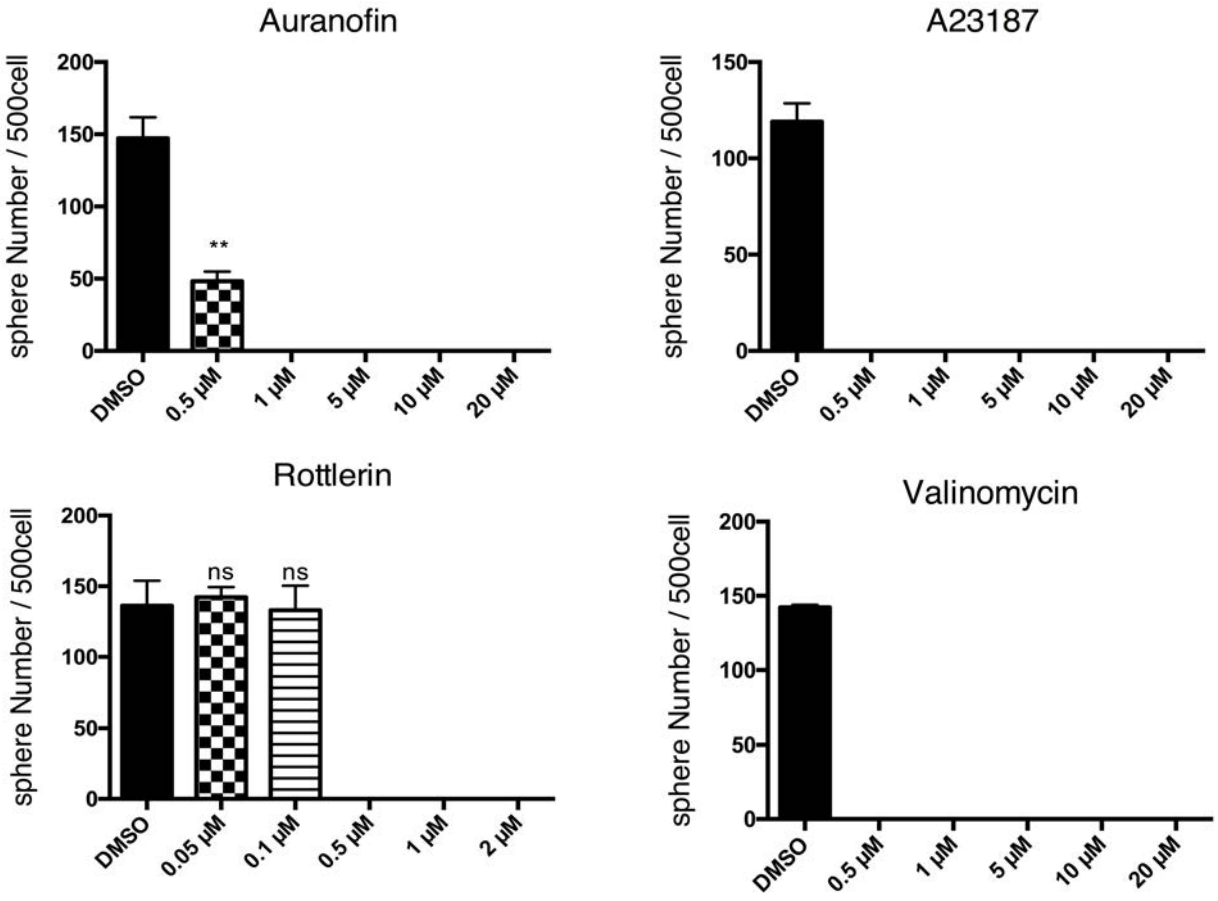

Figure 34. Therapeutic potential of other compounds for treatment of human GBM *in vitro*. Quantitation of sphere formation in TGS-04 human patient-derived GBM cells that were treated with the indicated concentrations of compounds. Data are the mean sphere number ± SD. n=3

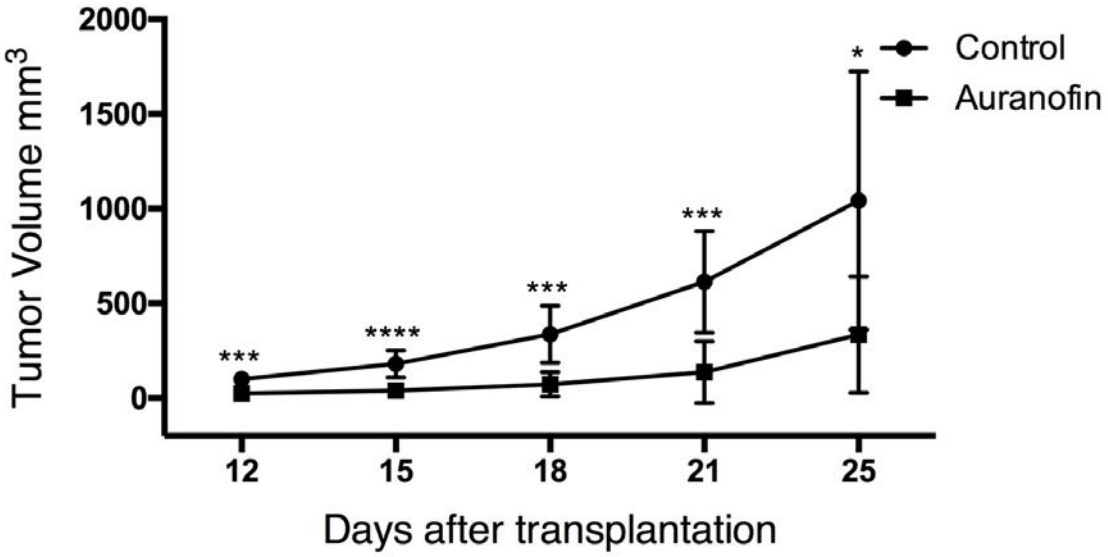

Figure 35. Therapeutic potential of auranofin for treatment of human GBM *in vivo*. Quantitation of volumes of tumors in the mice that had been subcutaneously inoculated with TGS-01 cells and treated with/without auranofin. Data are the mean volume ± SD for tumors from control (n=10) and auranofin-treated (n=8) mice. Statistical analyses were performed to detect differences between treated and untreated mice.

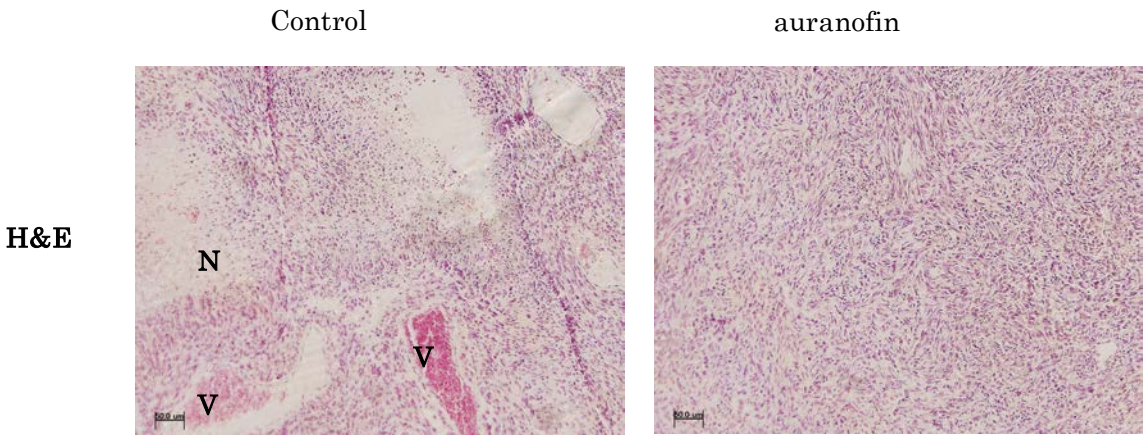

Figure 36. Immunohistochemical analysis of tumor sections after Nigericin treatment. Immunohistochemistry analyses of tumors that were isolated from the mice in (Fig.35) and subjected to HE staining. V and N indicate vasculature and necrotic area, respectively. Data are representative of 8 tumors examined/group. Scale bars, 50 μm.

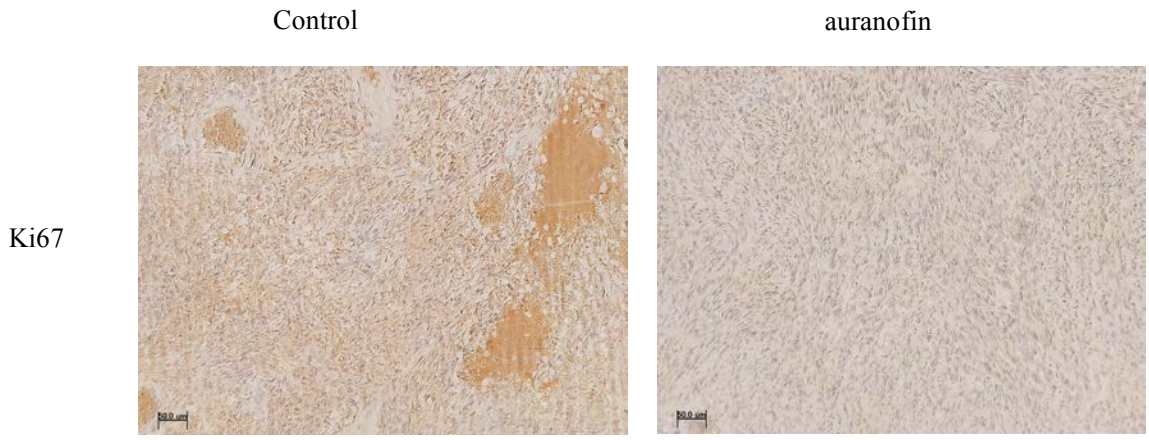

Figure 37. Immunohistochemical analysis of tumor sections after Nigericin treatment. Immunohistochemistry analyses of tumors that were isolated from the mice in (Fig.35) and subjected to immunostaining with Ki67 antibody. Data are representative of 8 tumors examined/group. Scale bars, 50 μm.

Discussion

There is much debate over the metabolic status of cancer stem cells in several types of tumors, including gliomas. One study reported that GICs are primarily glycolytic, and that pharmaceutical inhibition of glycolysis decreases the tumorigenicity of these cells(41). However, another study found that undifferentiated glioma cells show predominantly mitochondrial activity(42). These discrepancies may be due to fact that metabolic status is dynamic and easily influenced by factors critical for the determination of cancer cell fate, e.g. the cell-of-origin of the tumor, the types of gene mutations it bears, and the nutrient conditions in the surrounding microenvironment. This complexity makes it difficult to precisely define the role of metabolic regulation in a given cancer. This study focused on the relationship between metabolic status and mTOR signaling in glioma because mTORC1 hyperactivation correlates well with GBM patient prognosis (25-27) and found that mTORC1 hyperactivation increase energy dependence by mitochondrial OXPHOS. Although hyperactivation of mTORC1 is known to stimulate not only mitochondrial activity but also the

metabolism of lipids, nucleotides, and other cellular components, the data clearly indicate that enhanced bioenergetic capacity is crucial for expansion of GICs, supporting glioma malignancy.

Previously, Gupta *et.al.* developed a drug screening system to select specific inhibitors of breast cancer stem cells(43). In that study, mammalian epithelial cells were induced to transdifferentiate into a mesenchymal cell type by knock-down of E-cadherin. These cells acquired cancer stem cell properties, including a $CD44^{+}/CD24^{-}$ surface marker pattern, enhanced sphere formation capacity, and therapeutic resistance. Chemical screening for compounds that selectively killed mammalian epithelial cells exhibiting E-cadherin knock-down revealed that salinomycin (a K^{+} ionophore) suppressed mammary tumor growth and induced epithelial differentiation. Nigericin was also selected in that screening, although the effects of this agent were not fully characterized. Nigericin is a K^{+} ionophore that causes hyperpolarization of mitochondria, respiratory chain abnormalities and reduced ATP production(40,44). In addition, in a nasopharyngeal carcinoma cell line, nigericin treatment down-regulated expression of Bim1, a critical molecule supporting stem cell properties(45). Thus, like salinomycin,

nigericin appears to have selective effects on cancer stem cells. The identification of nigericin as an agent blocking the growth of mTORC1-driven mouse glioma cells demonstrates that the drug screening system used in this study is useful for isolating small molecule compounds capable of targeting cancer stem cells.

It is speculated that a therapeutic approach based on the specific targeting of mitochondrial ATP production would trigger a dramatic energy imbalance in mTOR-driven glioma cells. Since enhanced protein synthesis stimulated by mTORC1 activation induces an increase in ATP consumption due to heightened mRNA translation, disruption of this altered balance between ATP production and consumption by small molecule compounds such as oligomycin might lead to an energy crisis in mTORC1-driven glioma cells. It remains possible that nigericin and the other drug candidates selected by the screening process have effects in addition to their reduction of ATP levels that result in suppression of mTORC1-driven malignant phenotypes. For example, nigericin reportedly affects inflammasome activation (46), and such additional effects could conceivably contribute to suppression of tumor growth *in vivo.* Although its currently difficult to exclude this possibility for

individual agents, the fact that screening system in this study efficiently selected several compounds that induce mitochondrial abnormalities supports the hypothesis that targeting the altered energy balance in glioma cells has the potential to bring therapeutic benefits to glioma patients.

The biguanide metformin was originally used for treatment of diabetes mellitus but was recently found to have a potent tumor-suppressive effect that is independent of its anti-hyperglycemic function(11). A key outcome of metformin treatment is inhibition of mitochondrial complex I in the electron transport chain, which leads to an increase in the AMP/ATP ratio. This imbalance in turn induces activation of AMPK, a critical energy sensor that integrates multiple signaling pathways. In this study, results showed that, like metformin, nigericin induces AMPK activation associated with mTORC1 inhibition. Also the interesting possibility that disruption of a cell's energy balance may induce glioma cell differentiation mediated by AMPK activation was uncovered. On the other hand, more detailed evaluations of these observations are required for their translational application because nigericin administration did not greatly extend the survival of recipient mice bearing human GBM cells in the brain (Data not

shown), presumably due to the inability to penetrate the blood-brain barrier. Therefore, the characterization of individual compounds for their pharmacokinetics/pharmacodynamics in brain tissues is also important for any drug repositioning or drug repurposing designed to treat GBM patients. Further investigation is required to determine how these compounds exert tumor suppression, and to develop efficient anticancer therapeutics.

References

1. Cantor, J. R., and Sabatini, D. M. (2012) Cancer cell metabolism: one hallmark, many faces. *Cancer discovery* **2**, 881-898
2. Boroughs, L. K., and DeBerardinis, R. J. (2015) Metabolic pathways promoting cancer cell survival and growth. *Nature cell biology* **17**, 351-359
3. Vander Heiden, M. G., Cantley, L. C., and Thompson, C. B. (2009) Understanding the Warburg effect: the metabolic requirements of cell proliferation. *Science* **324**, 1029-1033
4. Hayashi, J., Takemitsu, M., and Nonaka, I. (1992) Recovery of the missing tumorigenicity in mitochondrial DNA-less HeLa cells by introduction of mitochondrial DNA from normal human cells. *Somatic cell and molecular genetics* **18**, 123-129
5. Cavalli, L. R., Varella-Garcia, M., and Liang, B. C. (1997) Diminished tumorigenic phenotype after depletion of mitochondrial DNA. *Cell growth & differentiation : the molecular biology journal of the American Association for Cancer Research* **8**, 1189-1198
6. Morais, R., Zinkewich-Peotti, K., Parent, M., Wang, H., Babai, F., and Zollinger, M. (1994) Tumor-forming ability in athymic nude mice of human cell lines devoid of

mitochondrial DNA. *Cancer research* **54**, 3889-3896

7. Tan, A. S., Baty, J. W., Dong, L. F., Bezawork-Geleta, A., Endaya, B., Goodwin, J., Bajzikova, M., Kovarova, J., Peterka, M., Yan, B., Pesdar, E. A., Sobol, M., Filimonenko, A., Stuart, S., Vondrusova, M., Kluckova, K., Sachaphibulkij, K., Rohlena, J., Hozak, P., Truksa, J., Eccles, D., Haupt, L. M., Griffiths, L. R., Neuzil, J., and Berridge, M. V. (2015) Mitochondrial genome acquisition restores respiratory function and tumorigenic potential of cancer cells without mitochondrial DNA. *Cell metabolism* **21**, 81-94
8. LeBleu, V. S., O'Connell, J. T., Gonzalez Herrera, K. N., Wikman, H., Pantel, K., Haigis, M. C., de Carvalho, F. M., Damascena, A., Domingos Chinen, L. T., Rocha, R. M., Asara, J. M., and Kalluri, R. (2014) PGC-1alpha mediates mitochondrial biogenesis and oxidative phosphorylation in cancer cells to promote metastasis. *Nature cell biology* **16**, 992-1003, 1001-1015
9. Viale, A., Pettazzoni, P., Lyssiotis, C. A., Ying, H., Sanchez, N., Marchesini, M., Carugo, A., Green, T., Seth, S., Giuliani, V., Kost-Alimova, M., Muller, F., Colla, S., Nezi, L., Genovese, G., Deem, A. K., Kapoor, A., Yao, W., Brunetto, E., Kang, Y., Yuan, M., Asara, J. M., Wang, Y. A., Heffernan, T. P., Kimmelman, A. C., Wang, H., Fleming, J. B., Cantley, L. C., DePinho, R. A., and Draetta, G. F. (2014) Oncogene ablation-

resistant pancreatic cancer cells depend on mitochondrial function. *Nature* **514**, 628-632

10. Roesch, A., Vultur, A., Bogeski, I., Wang, H., Zimmermann, K. M., Speicher, D., Korbel, C., Laschke, M. W., Gimotty, P. A., Philipp, S. E., Krause, E., Patzold, S., Villanueva, J., Krepler, C., Fukunaga-Kalabis, M., Hoth, M., Bastian, B. C., Vogt, T., and Herlyn, M. (2013) Overcoming intrinsic multidrug resistance in melanoma by blocking the mitochondrial respiratory chain of slow-cycling JARID1B(high) cells. *Cancer cell* **23**, 811-825
11. Foretz, M., Guigas, B., Bertrand, L., Pollak, M., and Viollet, B. (2014) Metformin: from mechanisms of action to therapies. *Cell metabolism* **20**, 953-966
12. Laplante, M., and Sabatini, D. M. (2012) mTOR signaling in growth control and disease. *Cell* **149**, 274-293
13. Wullschleger, S., Loewith, R., and Hall, M. N. (2006) TOR signaling in growth and metabolism. *Cell* **124**, 471-484
14. Hoshii, T., Matsuda, S., and Hirao, A. (2014) Pleiotropic roles of mTOR complexes in haemato-lymphopoiesis and leukemogenesis. *Journal of biochemistry* **156**, 73-83
15. Ramanathan, A., and Schreiber, S. L. (2009) Direct control of mitochondrial function by mTOR. *Proceedings of the National Academy of Sciences of the United States of America* **106**, 22229-22232

16. Cunningham, J. T., Rodgers, J. T., Arlow, D. H., Vazquez, F., Mootha, V. K., and Puigserver, P. (2007) mTOR controls mitochondrial oxidative function through a YY1-PGC-1alpha transcriptional complex. *Nature* **450**, 736-740

17. Morita, M., Gravel, S. P., Chenard, V., Sikstrom, K., Zheng, L., Alain, T., Gandin, V., Avizonis, D., Arguello, M., Zakaria, C., McLaughlan, S., Nouet, Y., Pause, A., Pollak, M., Gottlieb, E., Larsson, O., St-Pierre, J., Topisirovic, I., and Sonenberg, N. (2013) mTORC1 controls mitochondrial activity and biogenesis through 4E-BP-dependent translational regulation. *Cell metabolism* **18**, 698-711

18. Louis, D. N., Ohgaki, H., Wiestler, O. D., and Cavenee, W. K. (2007) WHO Classification of Tumours of the Central Nervous System 4th edn (eds Louis, D. N., Ohgaki, H., Wiestler, O.D. & Cavenee, W.K.) (World Health Organization, 2007).

19. Zhang, X., Zhang, W., Cao, W. D., Cheng, G., and Zhang, Y. Q. (2012) Glioblastoma multiforme: Molecular characterization and current treatment strategy (Review). *Exp Ther Med* **3**, 9-14

20. Reya T., Morrison SJ., Clarke MF., and IL., W. (2001) Stem cells, cancer, and cancer stem cells. *Nature* **414**, 105-111

21. Taipale J., and Beachy PA. (2001) The Hedgehog and Wnt signalling pathways in cancer. *Nature* **411**, 349-354

22. Pardal, R., Clarke, M. F., and Morrison, S. J. (2003) Applying the principles of stem-cell biology to cancer. *Nat Rev Cancer* **3**, 895-902

23. Singh, S. K., Hawkins, C., Clarke, I. D., Squire, J. A., Bayani, J., Hide, T., Henkelman, R. M., Cusimano, M. D., and Dirks, P. B. (2004) Identification of human brain tumour initiating cells. *Nature* **432**, 396-401

24. Brennan, C. W., Verhaak, R. G., McKenna, A., Campos, B., Noushmehr, H., Salama, S. R., Zheng, S., Chakravarty, D., Sanborn, J. Z., Berman, S. H., Beroukhim, R., Bernard, B., Wu, C. J., Genovese, G., Shmulevich, I., Barnholtz-Sloan, J., Zou, L., Vegesna, R., Shukla, S. A., Ciriello, G., Yung, W. K., Zhang, W., Sougnez, C., Mikkelsen, T., Aldape, K., Bigner, D. D., Van Meir, E. G., Prados, M., Sloan, A., Black, K. L., Eschbacher, J., Finocchiaro, G., Friedman, W., Andrews, D. W., Guha, A., Iacocca, M., O'Neill, B. P., Foltz, G., Myers, J., Weisenberger, D. J., Penny, R., Kucherlapati, R., Perou, C. M., Hayes, D. N., Gibbs, R., Marra, M., Mills, G. B., Lander, E., Spellman, P., Wilson, R., Sander, C., Weinstein, J., Meyerson, M., Gabriel, S., Laird, P. W., Haussler, D., Getz, G., Chin, L., and Network, T. R. (2013) The somatic genomic landscape of glioblastoma. *Cell* **155**, 462-477

25. Chakravarti, A., Zhai, G., Suzuki, Y., Sarkesh, S., Black, P. M., Muzikansky, A., and Loeffler, J. S. (2004) The prognostic

significance of phosphatidylinositol 3-kinase pathway activation in human gliomas. *Journal of clinical oncology : official journal of the American Society of Clinical Oncology* **22**, 1926-1933

26. Yang, J., Liao, D., Wang, Z., Liu, F., and Wu, G. (2011) Mammalian target of rapamycin signaling pathway contributes to glioma progression and patients' prognosis. *The Journal of surgical research* **168**, 97-102
27. Korkolopoulou, P., Levidou, G., El-Habr, E. A., Piperi, C., Adamopoulos, C., Samaras, V., Boviatsis, E., Thymara, I., Trigka, E. A., Sakellariou, S., Kavantzas, N., Patsouris, E., and Saetta, A. A. (2012) Phosphorylated 4E-binding protein 1 (p-4E-BP1): a novel prognostic marker in human astrocytomas. *Histopathology* **61**, 293-305
28. Thoreen, C. C., Kang, S. A., Chang, J. W., Liu, Q., Zhang, J., Gao, Y., Reichling, L. J., Sim, T., Sabatini, D. M., and Gray, N. S. (2009) An ATP-competitive mammalian target of rapamycin inhibitor reveals rapamycin-resistant functions of mTORC1. *The Journal of biological chemistry* **284**, 8023-8032
29. Yamada, D., Hoshii, T., Tanaka, S., Hegazy, A. M., Kobayashi, M., Tadokoro, Y., Ohta, K., Ueno, M., Ali, M. A., and Hirao, A. (2014) Loss of Tsc1 accelerates malignant gliomagenesis when combined with oncogenic signals. *Journal of*

biochemistry **155**, 227-233

30. Tuveson, D. A., Shaw, A. T., Willis, N. A., Silver, D. P., Jackson, E. L., Chang, S., Mercer, K. L., Grochow, R., Hock, H., Crowley, D., Hingorani, S. R., Zaks, T., King, C., Jacobetz, M. A., Wang, L., Bronson, R. T., Orkin, S. H., DePinho, R. A., and Jacks, T. (2004) Endogenous oncogenic K-ras(G12D) stimulates proliferation and widespread neoplastic and developmental defects. *Cancer cell* **5**, 375-387
31. Serrano, M., Lee, H., Chin, L., Cordon-Cardo, C., Beach, D., and DePinho, R. A. (1996) Role of the INK4a locus in tumor suppression and cell mortality. *Cell* **85**, 27-37
32. Tamase, A., Muraguchi, T., Naka, K., Tanaka, S., Kinoshita, M., Hoshii, T., Ohmura, M., Shugo, H., Ooshio, T., Nakada, M., Sawamoto, K., Onodera, M., Matsumoto, K., Oshima, M., Asano, M., Saya, H., Okano, H., Suda, T., Hamada, J., and Hirao, A. (2009) Identification of tumor-initiating cells in a highly aggressive brain tumor using promoter activity of nucleostemin. *Proceedings of the National Academy of Sciences of the United States of America* **106**, 17163-17168
33. Ikushima, H., Todo, T., Ino, Y., Takahashi, M., Miyazawa, K., and Miyazono, K. (2009) Autocrine TGF-beta signaling maintains tumorigenicity of glioma-initiating cells through Sry-related HMG-box factors. *Cell stem cell* **5**, 504-514
34. Soga, T., Ohashi, Y., Ueno, Y., Naraoka, H., Tomita, M., and

Nishioka, T. (2003) Quantitative metabolome analysis using capillary electrophoresis mass spectrometry. *J Proteome Res* **2**, 488-494

35. Soga, T., Baran, R., Suematsu, M., Ueno, Y., Ikeda, S., Sakurakawa, T., Kakazu, Y., Ishikawa, T., Robert, M., Nishioka, T., and Tomita, M. (2006) Differential metabolomics reveals ophthalmic acid as an oxidative stress biomarker indicating hepatic glutathione consumption. *The Journal of biological chemistry* **281**, 16768-16776
36. Hoshii, T., Tadokoro, Y., Naka, K., Ooshio, T., Muraguchi, T., Sugiyama, N., Soga, T., Araki, K., Yamamura, K., and Hirao, A. (2012) mTORC1 is essential for leukemia propagation but not stem cell self-renewal. *J Clin Invest* **122**, 2114-2129
37. Tanaka, S., Nakada, M., Yamada, D., Nakano, I., Todo, T., Ino, Y., Hoshii, T., Tadokoro, Y., Ohta, K., Ali, M. A., Hayashi, Y., Hamada, J., and Hirao, A. (2015) Strong therapeutic potential of gamma-secretase inhibitor MRK003 for CD44-high and CD133-low glioblastoma initiating cells. *Journal of neuro-oncology* **121**, 239-250
38. Nicholls, D. G. (2006) Simultaneous monitoring of ionophore- and inhibitor-mediated plasma and mitochondrial membrane potential changes in cultured neurons. *The Journal of biological chemistry* **281**, 14864-14874
39. Rigobello, M. P., Scutari, G., Boscolo, R., and Bindoli, A.

(2002) Induction of mitochondrial permeability transition by auranofin, a gold(I)-phosphine derivative. *British journal of pharmacology* **136**, 1162-1168

40. Manago, A., Leanza, L., Carraretto, L., Sassi, N., Grancara, S., Quintana-Cabrera, R., Trimarco, V., Toninello, A., Scorrano, L., Trentin, L., Semenzato, G., Gulbins, E., Zoratti, M., and Szabo, I. (2015) Early effects of the antineoplastic agent salinomycin on mitochondrial function. *Cell death & disease* **6**, e1930
41. Zhou, Y., Zhou, Y., Shingu, T., Feng, L., Chen, Z., Ogasawara, M., Keating, M. J., Kondo, S., and Huang, P. (2011) Metabolic alterations in highly tumorigenic glioblastoma cells: preference for hypoxia and high dependency on glycolysis. *The Journal of biological chemistry* **286**, 32843-32853
42. Vlashi, E., Lagadec, C., Vergnes, L., Matsutani, T., Masui, K., Poulou, M., Popescu, R., Della Donna, L., Evers, P., Dekmezian, C., Reue, K., Christofk, H., Mischel, P. S., and Pajonk, F. (2011) Metabolic state of glioma stem cells and nontumorigenic cells. *Proceedings of the National Academy of Sciences of the United States of America* **108**, 16062-16067
43. Gupta, P. B., Onder, T. T., Jiang, G., Tao, K., Kuperwasser, C., Weinberg, R. A., and Lander, E. S. (2009) Identification of selective inhibitors of cancer stem cells by high-throughput screening. *Cell* **138**, 645-659

44. Heid, M. E., Keyel, P. A., Kamga, C., Shiva, S., Watkins, S. C., and Salter, R. D. (2013) Mitochondrial reactive oxygen species induces NLRP3-dependent lysosomal damage and inflammasome activation. *Journal of immunology* **191**, 5230-5238

45. Deng, C. C., Liang, Y., Wu, M. S., Feng, F. T., Hu, W. R., Chen, L. Z., Feng, Q. S., Bei, J. X., and Zeng, Y. X. (2013) Nigericin selectively targets cancer stem cells in nasopharyngeal carcinoma. *The international journal of biochemistry & cell biology* **45**, 1997-2006

46. Munoz-Planillo, R., Kuffa, P., Martinez-Colon, G., Smith, B. L., Rajendiran, T. M., and Nunez, G. (2013) K(+) efflux is the common trigger of NLRP3 inflammasome activation by bacterial toxins and particulate matter. *Immunity* **38**, 1142-1153

Conclusion

In the present study, I investigated the molecular mechanism by which mTORC1 hyperactivation causes the malignant phenotypes of glioma cells. Results showed that mTORC1 hyperactivation promotes mitochondrial energy production, which in turn supports GIC expansion. Importantly, using this unique mTORC1-driven glioma model and drug screening system to identify small molecule compounds that may be effective for GBM therapy.

In this study, several compounds able to inhibit the mitochondrial activity were identified, these compounds reduced ATP levels remarkably and inhibited glioma sphere formation. In human patient-derived glioma cells TGS-01, Nigericin, which reportedly in previous studies to reduce cancer stem cell properties, induced AMPK phosphorylation, associated with mTORC1 inactivation, leading to a clear decrease of glioma sphere formation. Furthermore, histological and immunohistochemical analysis showed that malignant characteristics of human glioma cells were remarkably suppressed by nigericin treatment *in vivo*. Thus, targeting

mTORC1-driven processes, especially those involved in maintaining a cancer cell's energy balance, may be an effective strategy for glioma patients treatment.

Further investigation is required to determine how these compounds exert tumor suppression, and to develop efficient anticancer therapeutics targeting the altered energy balance in tumor cells.